# FINAL SCIENTIFIC REPORT (FSR) FOR DOE/EERE

|  |  |
|---|---|
| **Project Title:** | "Recovery Act: Advanced Building Insulation by the $CO_2$ Foaming Process" |
| **Covering Period:** | October 1, 2010 to December 31, 2013 |
| **Approved Project Period:** | October 1, 2010 to December 31, 2013 |
| **Submission Date:** | December 30, 2013 |
| **Recipient:** | Industrial Science & Technology Network, Inc.<br>1200 Corporate Blvd., STE 10C<br>Lancaster, PA 17601-1292 |
| **Website:** | http://www.istninc.com |
| **Award Number:** | DE-EE0003983 |
| **Working Partners:** | N/A |
| **Cost-Sharing Partners:** | N/A |
| **PI:** | Dr. Arthur J. Yang<br>President and CTO<br>Industrial Science & Technology Network, Inc.<br>Phone: 717-522-1739<br>Fax: 717-522-1319<br>Email: ajyang@istninc.com |
| **Submitted by:** | Dr. Arthur J. Yang |
| **DOE Project Team:** | DOE Project Officer – Leon Fabick<br>DOE Project Officer – Jim Payne |

December 30, 2013

Signature Date

*Acknowledgment: "This material is based upon work supported by the Department of Energy under Award Number DE-EE0003983."*

# Table of Contents

# 1. Executive Summary

## Background

Thermal building insulation is among the most important solutions to the global energy crisis. According to the U.S. Energy Information Administration, new energy generation requires an investment of $3,362/kW for a fossil-energy plant, and $5,530/kW for a nuclear power plant. In contrast, the application of thermal building insulation reduces energy consumption at an investment of only $125/kW. This low cost highlights the importance of insulation materials in building structures, which are responsible for 40% of global energy consumption and 24% of carbon dioxide ("$CO_2$") emissions. Given such intensive energy use, an improvement in the thermal resistance, or R-value [1], of building insulation would reduce energy waste at a considerable level. However, the insulation industry is notoriously conservative and has not developed commercial R-value improvements in many decades. The current "2nd" generation of thermal insulation technology is almost 70 years old. A breakthrough in advanced materials would benefit energy efficiency significantly in the U.S., as well as developing markets such as China and India, where many buildings are poorly insulated despite rapidly growing populations and energy consumption.

The insulation industry's lack of innovation has created opportunities for technology disruption in several key market segments, such as extruded polystyrene ("XPS") [2]. XPS comprises a $5.1 billion worldwide market with two major needs: 1) higher R-value foams without cost increase, and 2) new foaming agents to replace environmentally damaging hydrofluorocarbons ("HFCs") in the production process. Improvement of R-values is a significant technological challenge because the current processing methods and raw materials mix have been optimized over many decades to produce the best R-value at the lowest cost. Also, while HFCs are necessary for high R-value, they have 1,300 times the global warming power of $CO_2$ – a risk that has driven numerous changes in international environmental policy, including bans of HFCs in many of the major industrialized countries over the next few years. These bans are a catalyst for significant increases in commercial demand of environmentally clean XPS, and would benefit early entrants that could establish a strategic market position for the introduction of higher R-value alternatives that significantly enhance future energy efficiency. The prevailing problem for existing manufacturers is that conversion to a $CO_2$ foaming process would result in R-values 20% lower than the current industry standard in HFC-foamed products.

## Project overview

In this project, ISTN proposed to develop a new "3rd" generation of insulation technology. The focus was a cost-effective foaming process that could be used to manufacture XPS and other extruded polymer foams using environmentally clean blowing agents, and ultimately achieve higher R-values than existing products while maintaining the same level of cost-efficiency. In the U.S., state-of-the-art products are primarily manufactured by two companies: Dow and Owens

---

[1] R-value (thermal resistance) is a common measure of insulation value, equivalent to the reciprocal of thermal conductivity in units of $ft.^2 \cdot °F \cdot hr./Btu$. R-5/inch insulation with 3-inch thickness has a total R-value of 15. R-values in this document assume temperature of 75°F.

[2] XPS is a rigid foam board with widespread use in wall sheathing and foundational components due to a high R-value, rigid structure, and cost-efficiency. The manufacturing process uses extruders to expand a mixture of molten PS resin with HFC foaming agents into sheets of low density, closed cell foam. XPS annual sales are $1.1B in the U.S. (12% of U.S. market) and $5.0B worldwide.

Corning. These products (i.e., STYROFOAM and FOAMULAR) have a starting thermal resistance of R-5.0/inch, which declines over the life of the product as the HFC blowing agents essential to high R-value exchange with air in the environment. In the existing technologies, the substitution of $CO_2$ for HFCs as the primary foaming agent results in a much lower starting R-value, as evidenced in $CO_2$-foamed varieties of XPS in Europe with R-4.2/inch insulation value.

**The major overarching achievement from this project was ISTN's development of a new process that uses $CO_2$ as a clean blowing agent to achieve up to R-5.2/inch at the manufacturing scale, with a production cost on a per unit basis [3] that is less than the cost of Dow and Owens Corning XPS products.**

From the outset, this project was designed to create a super-thermal, nanopore insulation using a set of novel innovations that can be integrated into the foam extrusion process utilized in XPS manufacturing, giving high-throughput production and optimal cost-efficiency. Previous attempts in the industry to develop super-thermal nanopore insulations were not useful to applications in the building envelope because their high R-values required the use of supercritical drying, which is a batch production process with exceedingly high costs. Our intent was to make similar improvements in the material technology, but using a production process that is cost-efficient (extrusion) and clean ($CO_2$ blowing agent). By accomplishing the major goal of a highly competitive building insulation product that replaces high global-warming HFCs in production, this project was able to create a product that meets DOE and ARRA goals of enhancing U.S. energy efficiency, sustainability and manufacturing job opportunities. Further, we demonstrated the potential for implementing other technology enhancements in full-scale production to significantly raise insulation value in future versions of commercial product.

### Technical goals and accomplishments

There were four key technical objectives in ISTN's project:

(a) <u>Clean blowing agent</u> – Using $CO_2$ as the main blowing agent to foam building insulation, resulting in a cleaner process with significantly lower emissions than the current HFC-based methods;

(b) <u>Pore morphology and orientation</u> – Growing oblate pore (short polar axis and long equator axes, i.e. disk-like) morphology and orienting pores in a preferred direction to lower density and increase both insulation value and cost-efficiency;

(c) <u>Radiation blockers</u> – Using aligned reflecting surfaces to block radiation heat loss and further optimize insulation value;

(d) <u>Secondary nanostructure</u> – Creating secondary nanostructure within asymmetrical air pores to demonstrate the potential for major (>50%) increases in insulation values, which have remained stagnant in the building insulation industry for several decades.

We sought to examine and explore these four elements starting at the laboratory level, then moving into pilot production, and then eventually full-scale production so that the result would be a commercially viable product, with a technology platform for future generations of product with significantly enhanced performance. ISTN's major innovation was utilizing the creation of oriented anisotropic pore structure to substantially increase insulation value in the heat flow direction at the

---

[3] \$/R/board-ft. is the relevant metric for comparing insulation costs on an R-value adjusted, per unit basis. R-5/inch insulation that costs \$0.35/board-ft. has an R-value adjusted cost of \$0.07/R/board-ft. A board-ft. is 12 in. x 12 in. with 1-inch thickness.

expense of reduced insulation in the two irrelevant directions. Major technical accomplishments of the project are summarized below:

(1) By achieving both objectives (a) and (c) at the production scale, we demonstrated that R-5/inch building insulation can be manufactured without using any harmful blowing agents, and thus, have accomplished the most important goal of this project (the elimination of high global-warming reagents such as HFCs in the production of R-5/inch building foam insulation at a market acceptable cost).

(2) In our full-production factory test, we achieved the control of pore geometry and orientation in the $CO_2$ foam extrusion process and thus are capable of further improving the foam insulation value to R-6/inch with the appropriate modification of the extruder die design. The specific results and the design of a new die were submitted for the filing of a new patent.

(3) The creation of the secondary nanopore structure in a foaming process is still being improved at the laboratory and pilot level with our invention of a new polymer surfactant in assisting the required homogeneous nucleation. The continuation of this work towards the production of R-7~10/inch super thermal insulation in a foaming process is our next technical objective following this project.

A summary of key product performance results from the factory trials in this project are included below:

|  |  |  | Total | R-value |  | Density | Porosity | Avg. cell |
|---|---|---|---|---|---|---|---|---|
| **Start date** | **Trial** | **Location** | **output (kg)** | **Initial** | **1-year** | **($kg/m^3$)** | **(%)** | **size (µm)** |
| 12/06/11 | MuCell | Woburn, MA | 45 | 4.59 | 4.55 | 37.3 | 96.5% | 73.0 |
| 02/14/12 | MuCell | Woburn, MA | 45 | 5.21 | 4.73 | 41.0 | 96.1% | 50.0 |
| 10/20/12 | Hoswell | Shanghai | 427 | 5.17 | NA | 32.6 | 96.9% | 116.0 |
| 10/20/12 | Hoswell | Shanghai | 427 | 4.97 | NA | 32.6 | 96.9% | 94.0 |

**Table 1. Summary of product performance in ISTN-run factory trials.**

## Energy, environmental and economic benefits

Our technical achievement in producing insulation with the highest R-value via $CO_2$ foaming will allow all building insulation manufacturing to replace the use of HCFCs and HFCs, generating a huge environmental benefit of eliminating both ozone depleting and high global warming power emissions. The below table compares the global warming power of $CO_2$ to the most common blowing agents for XPS. As an example, blowing agents comprise an average of 15% of XPS materials, so 1 metric ton of today's XPS would require approximately 150kg of HFC-134a. This total has an emissions impact of 195,000 kg of $CO_2$. In contrast, a $CO_2$-foamed product would have an emissions impact of only 150 kg (i.e., a 99.9% reduction in emissions).

| Source | $CO_2$ | HFC-134a | HCFC-142b |
|---|---|---|---|
| GWP100 | 1 | 1,300 | 2,000 |

**Table 2. Global Warming Potential ("GWP") Values [4].**

We have modeled conservatively that the technology platform developed in this project could achieve 12% penetration of the U.S. building insulation market within 10 years. In this case, our

---

[4] U.S. Environmental Protection Agency, “Greenhouse Gases and Global Warming Potential Values”, Excerpt from the Inventory of U.S. Greenhouse Emissions and Sinks: 1990-2000, U.S. Greenhouse Gas Inventory Program, Office of Atmospheric Programs, EPA 430-R-02-003, Washington, DC, April, 2002.

products will provide domestic energy savings of 341 trillion BTU per year. $CO_2$ emissions savings will be 31.7 million metric tons per year, with 20.4 million metric tons due to the reduced energy waste, and 11.2 million metric tons due to replacing HFCs with $CO_2$ in foaming production. The emissions savings equate to removing 6.7 million cars from the road or 2.9 million fewer homes consuming energy. Overall, the total annual economic savings will be $8.7 billion, with $7.5 billion from reduced energy waste and $1.2 billion from reduced $CO_2$ emissions.

**Platform for future development**

Over a three-year project timeline, our proposed objectives and development work led to the creation of an advanced platform for foam insulation. The current, commercial-ready version of the product has performance and production costs equal to state-of-the-art XPS foams produced by Dow and Owens Corning. To capitalize on the potential environmental, energy and economic benefits of our technical success, we plan to pursue two concurrent paths for further development:

(1) <u>Improve insulation value by 50% or more</u> – At the end of this project, the $CO_2$-blown product ready for commercial production has comparable R-value to HFC-blown products, and approximately 20% better R-value than other $CO_2$-blown products. This already provides a commercial advantage as HFCs will eventually be phased out of production, requiring a clean substitute (i.e., ISTN's $CO_2$ technology). As important, modeling and theoretical bases of our new platform indicate that significant R-value improvements are possible with the proper integration of secondary nanostructures into new foam polymer blends. Thus, the development priority following this project is a next-generation foam insulation with 50% greater R-value and cost-efficiency, which altogether would revolutionize the building insulation market with a disruptive, best-in-class product.

(2) <u>Commercialization opportunities and market</u> – ISTN will carefully examine both licensing opportunities with larger commercial partners and the set-up of our own manufacturing business based on the technology platform. Outreach for licensing discussions will include foam manufacturing companies that do not specialize in XPS (XPS manufacturers represent a competitive risk given the exchange of information), as well as PS manufacturers interested in downstream derivative products. The pursuit of ISTN's own manufacturing business will include extensive evaluation of the market, intellectual property, and the assembly of a manufacturing and sales team.

The above-mentioned goals of raising insulation value and bringing the technology to the market as a commercial product together serve as the subject of a subsequent DOE grant project application.

# 2. Technical Background

The technology for present day ("2nd generation") thermal insulation foams is almost 70 years old. Since the entrapped, quiescent air within the foam is the best insulating medium, lowering the density (i.e. increasing the air content) leads to better insulating performance. 2nd generation products achieved improved R-values at greatly reduced cost using synthetic materials of densities much lower than natural insulation material ("1st generation"). However, the 2nd generation long ago reached its limit because excessive air inclusions compromised mechanical strength and, in fact, degraded the insulation value due to more radiation heat loss through the transparent air pockets.

Modeling and experimental results had demonstrated for some time that making the pore size close to or smaller than the mean free path [5] of air (~100 nm) could substantially reduce the thermal conductivity of the pore-entrapped air, leading to superior thermal insulations. This concept of "3rd generation" insulation – controlling pore size and morphology to further improve insulation value beyond density reduction – was first developed by the proposal team in the early 1990s while working on a grant-funded project from the Advanced Technology Program of NIST [6]. In this project, the team created prototype nanopore super insulation with R-values 3x better than fiberglass (comparison table below).

| Insulation Material | Thermal $\lambda$ (W/(m·K) x $10^{-3}$) | R-value-per-inch |
|---|---|---|
| *Fiberglass* | 45 | 3.2 |
| Granular Silica Aerogel | 23 | 6.3 |
| Aerogel with Layered Silicates Panels | 16 | 9 |
| Inverse-Emulsion Composite Panels | 20 | 7.2 |
| Aerogel-Polymer Microcomposites | 17 | 8.7 |
| Inorganic-Organic Composite Aerogel | 13 | 10.5 |

**Table 3. Comparison of aerogel insulations developed in ATP project to fiberglass standard.**

However, this novel approach solved only half of the problem in commercializing a super-thermal insulation. The combination of extremely high porosity and unprecedented small pore size in these nanopore insulations required very delicate processing. As good building insulations contain 95%+ air with low solid content, the processing and shipping costs become dominant factors in the cost structure pricing structure. Aerogels as developed in the ATP project use a batch production process that even today involves too much processing complexity and high costs to be commercialized beyond a niche scale. For example, Aspen, the largest aerogel company, projected 2014 worldwide sales of just under $100M, whereas XPS sales worldwide were projected to be over $5B.

In this project, we sought to improve on our previous work in aerogels and develop a commercially viable, **cost-effective foaming process for the production of the 3rd generation insulation**. As referenced above, previous nanopore insulations were made by a liquid sol-gel process and must be dried with supercritical $CO_2$ to preserve the fine pores. The drying process is a batch process, capital intensive, and extremely slow. In contrast, we designed our technology to use supercritical

---

[5] Mean free path: the average distance traveled by a molecule between two consecutive collisions.

[6] "Thermal Insulation Materials-Morphology Control and Process for the Next Generation of Performance", ATP (1992-1995).

$CO_2$ for the same purpose of minimizing surface tension (to help create and preserve small pores), but through a rapid foaming process such as extrusion to overcome prior manufacturing inefficiencies. Furthermore, we designed several innovations to boost insulating power in addition to what is accomplishable by pore size reduction. These additional options complement previous nanopore super insulation approaches but greatly reduce commercialization risk to improve the odds of success. Overall, the technical objectives of this project were:

(a) **Clean blowing agent** – Using $CO_2$ as the main blowing agent to foam building insulation;

(b) **Pore morphology and orientation** – Growing oblate pore (short polar axis and long equator axes, i.e. disk-like) morphology and orienting pores in a preferred direction;

(c) **Radiation blockers** – Using aligned reflecting surfaces to block radiation heat loss;

(d) **Secondary nanostructure** – Creating secondary nanostructure within asymmetrical air pores.

Our major innovation was to utilize the creation of oriented anisotropic pore structure to substantially **increase the insulation value in the heat flow direction at the expense of reduced insulation in the two irrelevant directions**, accomplishing the best utilization and balance of the composite properties. Our modeling results clearly showed that aligning oblate pores against the heat flow direction could reduce the composite thermal conductivity by 20% along the application direction; this gain in insulation value was just what a new insulation needs to break into the existing market. Moreover, the aligned oblate pores, having many layers of interfaces, could strongly **enhance radiation blocking**, effectively lifting the cap that has prevented further improvement by density reduction in 2nd generation approaches.

Adding innovations (b)-(d) to boost insulating power could greatly alleviate the risk of relying on processing a nanopore structure alone – which not only could help realize the cost-effective production of the advanced insulation by foaming, but also accomplish this goal by a progressive approach – and thus, is capable of hedging the risks of commercializing a revolutionary product. Incumbent HFC-blown building insulations have thermal conductivity of 29 mW/M·°K (R-5/inch). Simply replacing the HFC blowing agents with $CO_2$ (the best clean alternative) would lead to foam with inferior insulation value at R-4.2/inch (34 mW/M·°K). Our proposed enhancement strategy was designed to progressively reduce the thermal conductivity from 34 to 26 mW/M·°K by implementing innovation (b), further down to 21 mW/M·°K with elimination of radiation loss by (c), and eventually arrive at a super insulation value of 15 mW/M·°K (R-9.6/inch) after successfully creating the secondary nanostructure of (d). In terms of R-value, implementing the three innovations (b, c, d) could theoretically improve $CO_2$-foamed R-value to the state-of-the-art R-5/inch, then to R-7/inch, and eventually to R-9.6/inch. The goal of this project was to develop the technology platform and achieve the initial (arguably most difficult) jump to an R-5/inch $CO_2$-foamed XPS insulation.

### State-of-the-art and existing products

Both at the outset and end of this project, commercial building insulations had not been improved for many decades. Fiberglass (R-3.2/inch) is used between wall studs and XPS or urethane foam insulation (R-5/inch) is applied as outside sheathing to enhance wall R-value to above 16. Although fiberglass is inferior in insulation value and mechanical strength, it is used commonly between wall studs because of lower cost. Any replacement insulation, even with better insulating power, must still compete on the basis of cost-per-R-value, in which fiberglass is usually advantageous. The need to be cost-competitive dictated our desire for creating an enhanced foam extrusion process, as the high throughput rate of extrusion and resultant low densities of the foams are key drivers in good cost-efficiency. With processing costs in check, any R-value enhancement achieved by our technology could immediately lead to significant market penetration.

Further, we proposed $CO_2$ foaming specifically to provide the significant and near-immediate benefit of reducing harmful gas emissions during production, as currently-used HFC blowing agents have 1,300x the global warming potential of $CO_2$. The XPS industry has already previously moved from hydrochlorofluorocarbons ("HCFCs") to HFCs, as the former were banned in 2010. HFCs continue to be used commonly in XPS production and as refrigerants, among many other applications, but will eventually be banned as well in favor of $CO_2$. The dilemma for the insulation industry is that HCFCs and HFCs have intrinsically lower thermal conductivity, which gives a temporarily higher insulation value (R-5/inch) before dropping to R-4.2/inch after replacement by air (within 6 to 12 months). Meanwhile, the use of $CO_2$ in incumbent XPS technologies gives a lower starting point of approximately R-4.2/inch.

# 3. Project Objectives

## Approach

Affordable, high performance, thermal insulation is the single technology that can have a major impact on both of the key energy-related national problems – energy shortage and global warming. In this project, we proposed to develop a new generation of thermal insulation with substantially higher insulating power (higher R/inch) at an affordable cost. The key to our approach was a conventional foaming process that produces rigid polymer-clay nanocomposite foam with pore sizes several orders of magnitude smaller combined with an aligned oblate pore structure, and embedded with a secondary structure in the nanometer range to substantially increase the R/inch values. The technology development of this project led to the creation of a platform for manufacturing XPS with competitive performance and costs using CO2 as a clean blowing agent replacement for HFCs, and will eventually lead to the production of a 3rd generation insulation with insulating power 50-100% higher than current products (R-7~10/inch versus current R-3.2 ~5/inch), with costs still commensurate to present market demands. The new technology will not only revitalize the stagnant insulation industry, but also create enormous economic and environmental benefits.

## Design of tasks and progression timeline

As discussed above, our work plan correlated R-value improvements with four technical goals:

(a) **Clean blowing agent** – Using $CO_2$ as the main blowing agent to foam building insulation;

(b) **Pore morphology and orientation** – Growing oblate pore (short polar axis and long equator axes, i.e. disk-like) morphology and orienting pores in a preferred direction;

(c) **Radiation blockers** – Using aligned reflecting surfaces to block radiation heat loss;

(d) **Secondary nanostructure** – Creating secondary nanostructure within asymmetrical air pores.

The proposed work plan had established the following check points of technology progress milestones over the project periods: **6 months**: Laboratory prototypes of **(a)** and **(b)**, **12 month**: Laboratory prototype of **(c)**, **15 month**: Pilot demonstration of **(a)**, **21 month**: Pilot demonstration of **(b)**, **24 months**: Laboratory prototypes of **(d)**, **27 month**: Pilot demonstration of **(c)**, **36 month**: Pilot demonstration of **(d)**.

| Task | Key property | Additional attributes |
|---|---|---|
| a. Smaller pores and radiation blocking | R-5/inch | Pore size < 10 μ, density ~ 0.03g/cc |
| b. Oblate pores and radiation blocking | R-6/inch | Aspect ratio ~ 10, density ~ 0.03g/cc |
| c. Orientation of oblate pore structure | R-6~8/inch | Pores aligned, density ~ 0.03g/cc |
| d. Creating nanostructure within pores | R-8~10/inch | Nanopore structure within oblate pores |

**Table 4. Design of tasks and progression timeline**

| Quarter: | 1 | 2 | 3 | 4 | 5 | 6 | 7 | 8 | 9 | 10 | 11 | 12 |
|---|---|---|---|---|---|---|---|---|---|---|---|---|
| **(a) Using $CO_2$ as the main blowing agent to foam building insulation** | | | | | | | | | | | | |
| (a.1) $CO_2$ solubility enhancement | ■ | ■ | ■ | | | | | | | | | |
| (a.2) Homogenous nucleation | | ■ | ■ | ■ | ■ | | | | | | | |
| (a.3) Rheology control | | | ■ | ■ | ■ | ■ | ■ | ■ | ■ | ■ | | |
| **(b) Growing and orienting oblate Pores** | | | | | | | | | | | | |
| (b.1) Pressure vessel $CO_2$ foaming | | ■ | ■ | ■ | ■ | | | | | | | |

| | | | | | | | | | | | | |
|---|---|---|---|---|---|---|---|---|---|---|---|---|
| (b.2) Pilot-scale extrusion experiments | | | ▨ | ▨ | ▨ | ▨ | ▨ | ▨ | ▨ | ▨ | ▨ | ▨ |
| (b.3) Oblate pores by injection molding | | | | | | ▨ | ▨ | ▨ | ▨ | ▨ | ▨ | ▨ |
| **(c) Using aligned reflecting surfaces to block radiation heat loss** | | | | | | | | | | | | |
| Exfoliated clay, graphite, Al flakes | | ▨ | ▨ | ▨ | ▨ | ▨ | ▨ | ▨ | ▨ | | | |
| **(d) Creating the secondary nanopore structure within oblate pores** | | | | | | | | | | | | |
| (d.1) Surface incorporated structure | ▨ | ▨ | ▨ | ▨ | ▨ | ▨ | ▨ | ▨ | ▨ | | | |
| (d.2) Intertwined structure within pores | | | | | ▨ | ▨ | ▨ | ▨ | ▨ | ▨ | ▨ | ▨ |

**Table 5. Timeline of development.**

# 4. Project Results and Discussion

This project was designed to maximize the commercial and energy benefits achievable during the three year project timeline and budget. The grant resources were strategically distributed among the three phases of the designed work plan and tasks, namely the (laboratory) pressure vessel experiments, the (pilot) low-throughput extruder runs, and lastly, the (factory) manufacturing-scale production trials in order to commercialize an advanced insulation with competitive performance/cost ratio. The following results include detailed discussion of the project objectives as organized by the three categories above (i.e. sequentially from early-stage to manufacturing-stage), and the relevant project results and data.

## A. Pressure Vessel Experimental Design and Results

### ISTN pressure vessel set-up

We designed and constructed a pressure vessel that was used to prepare foam insulation samples using carbon dioxide as a blowing agent. An important feature of the vessel design was to allow foam expansion substantially more in the lateral direction which could create disk-shaped pore structures and also produce lower density foams. The equipment had been utilized throughout the project to produce test foam insulation with several different polymer bases and a variety of additives as well as blends. It allowed foaming with 100% $CO_2$ blowing agent up to 200°C and 2000 psi (138 bar). We designed the equipment for producing samples of an appropriate size and shape (100mm x 150mm) suitable for the direct thermal conductivity measurement using ISTN's thin-foil apparatus. The figure below illustrates the design and setup.

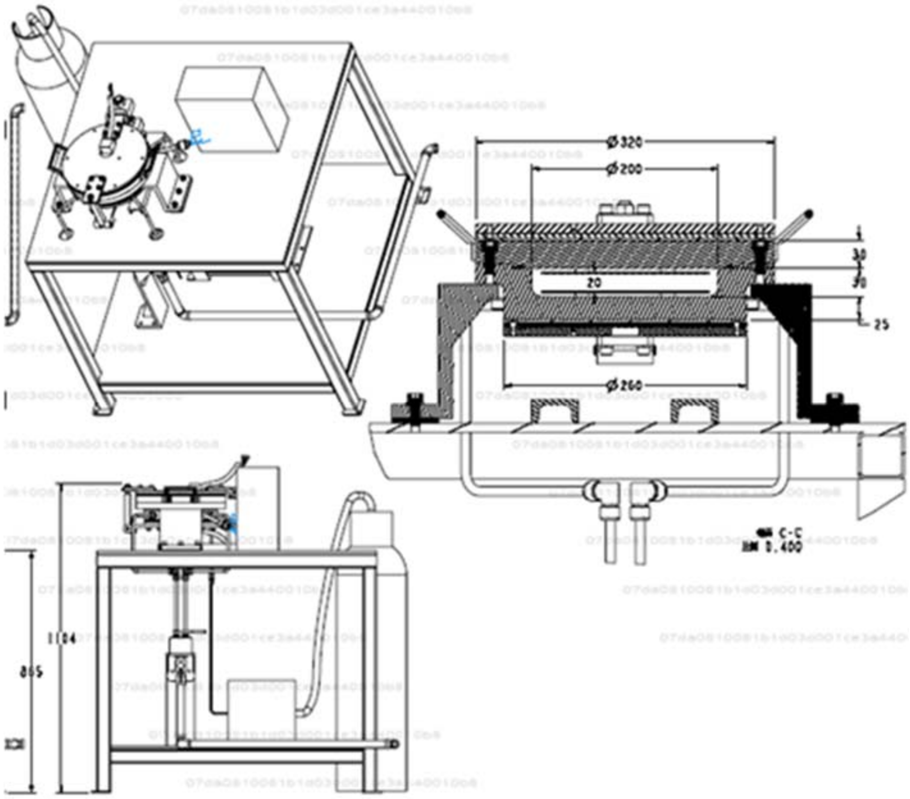

**Figure 1. ISTN pressure vessel set-up**

Compared with a conventional foaming vessel, our new design allows a much faster pressure relief (~100 bar/sec), which improved our capability of inducing homogeneous gas bubble nucleation prior to expansion of the gas laden polymer melt. By enhancing homogeneous nucleation, we may reduce cell pore size of foam. Preliminary foam samples were made using a conventional pressure vessel at the Ohio State University and then repeated with ISTN's pressure vessel. We achieved lower foam densities compared to the conventional vessel.

The following are photographs of the specially designed vessel intended for making large, flat foamed insulation samples suitable for thermal conductivity evaluation.

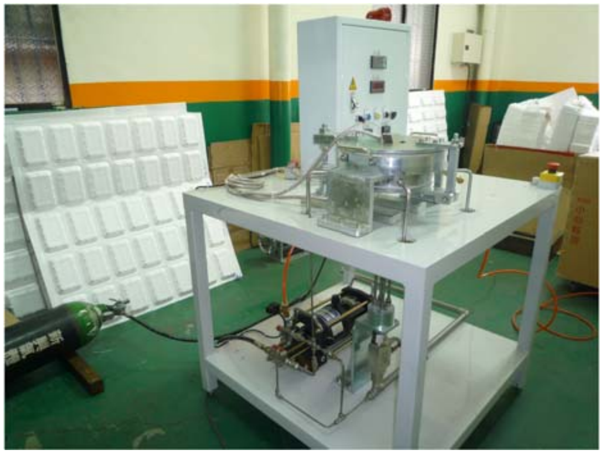

**Figure 2. ISTN pressure vessel.**

**Figure 3. ISTN pressure vessel close-up.**

Foaming conditions of candidate polymer formulations were assessed and used in the pilot extrusion phase of experiments. Batches of the polystyrene and polymer masterbatch - additive mixtures were generally made using a twin screw extruder equipped with a pelletizer. Suitable disc shaped plaques (10mm and 7mm thick) for foaming in the pressure vessel were made by injection molding. The pressure vessel was heated to the experimental temperature and filled with supercritical $CO_2$ up to the desired pressure using a high-pressure pump. The internal volume of the vessel was one liter. The vessel was then maintained at the desired pressure and temperature for up to 48 hours. The temperature was then lowered to the desired foaming temperature and the vessel was depressurized to atmospheric pressure at a rate of between 20 - 120 bar/second, while holding the temperature constant. Then the vessel was opened quickly, and the sample was removed for characterization.

Since the major issue of making a cost-competitive thermal insulation is its density reduction, we focused our majority efforts in making the lowest possible density of each recipe whenever possible. The following tables illustrates selected results of the pressure vessel foaming experiments.

## Data and Analysis of ISTN Pressure Vessel Foaming Experiments

| Sample | Disc Thickness mm | Soak T, P | Foaming T, P | Release Timing (s) | Foam Density kg/m$^3$ | Dimension |
|---|---|---|---|---|---|---|
| Pure PS | 10 | 130 °C 110 bar 48 hr | 130 °C 110 bar | 1 - 2 | 74.6 | |
| ISTN3-2 | 10 | 145 °C 110 bar 48 hr | 120 °C 110 bar | 1&10 | 48.2 | 180x8~10 mm |
| ISTN3-4 | 10 | 145 °C 110 bar 48 hr | 128 °C 110 bar | 1&10 | 74.4 | 125-145x7~12 |
| ISTN3-2B | 10 | 135 °C **120** bar 48 hr | 120 °C **120** bar | 1&12 | 46.3 | 160- |
| ISTN3-3 | 10 | 135 °C 110 bar 48 hr | 120 °C 110 bar | 5 | 46.3 | 155- |
| ISTN3-5 | 10 | 135 °C 110 bar 48 hr | **118** °C 110 bar | 5 | 43 | 180 x 8~13mm |
| ISTN3-7 | 10 | 135 °C 110 bar 48 hr | **118** °C 110 bar | 3 | 61 | 157-162x7~15 |
| ISTN4-1A | 7 | 135 °C 110 bar 24 hr | **120** °C 110 bar | 3 | 41.1 | 122-125 x13~24 |
| ISTN3-12 | 10 | 135 °C 110 bar 48 hr | **120** °C 110 bar | 3 | 40.8 | 135-138x16~24 |
| ISTN4-1B | 7 | 135 °C 110 bar 24 hr | **122** °C 110 bar | 1 | 41.4 | 117-126 x11~24 |
| ISTN4-1C | 7 | 135 °C 110 bar 24 hr | **122** °C 110 bar | 3 | 42.8 | 118-122 x14~22 |
| ISTN4-2B | 7 | 135 °C 110 bar 24 hr | **121** °C 110 bar | 3 | 50.4 | 117-119 x12~19 |
| ISTN4-2A | 7 | 135 °C 110 bar 24 hr | **119** °C 110 bar | 3 | 48.5 | 121-124 x13~19 |
| ISTN4-2C | 7 | 135 °C 110 bar 24 hr | **117** °C 110 bar | 3 | 57.3 | 112-114 x12~18 |
| ISTN4-3C | 7 | 135 °C 110 bar 24 hr | **119** °C 110 bar | 1 | 44.3 | 133-136 x11~17 |
| ISTN4-3B | 7 | 135 °C 110 bar 24 hr | **121** °C 110 bar | 1 | 38.4 | 142-146 x14~18 |
| ISTN4-5A | 7 | 135 °C 110 bar 24 hr | **122** °C 110 bar | 1 | 37.2 | 134-142 x10~20 |
| ISTN4-5C | 7 | 135 °C 120 bar 24 hr | **122** °C 120 bar | 1 | 35.4 | 134-141 x10~19 |
| ISTN3-8 | 10 | 130 °C 125 bar 48 hr | **121** °C 125 bar | 1 | 33 | 132-193x11-15 |
| ISTN3-14 | 10 | 130 °C 125 bar 48 hr | **121** °C 125 bar | 1 | 47 | 147-161x8.5-18 |
| ISTN5-2A | 7 | 130 °C 120 bar 24 hr | **122** °C 120 bar | 1 | 49.5 | 115~128 x 9~20 |
| ISTN5-2C | 7 | 135 °C 120 bar 22 hr | **122** °C 120 bar | 1 | 35 | 135-155 x 9~20 |
| ISTN5-2B | 7 | 135 °C 120 bar 22 hr | **121** °C 120 bar | 1 | 34.6 | 144-162 x 8~22 |
| ISTN5-3C | 7 | 135 °C 120 bar 22 hr | **121** °C 120 bar | 1 | 38.7 | 137~149 x 9~14 |
| ISTN5-3A | 7 | 135 °C 120 bar 22 hr | **122** °C 120 bar | 1 | 34.8 | 149-156 x 11~13 |
| ISTN5-3B | 7 | 135 °C 120 bar 22 hr | **122** °C 120 bar | 1 | 36.4 | 144-161 x 11~15 |

**Table 6. ISTN Pressure Vessel Foaming Experiments Data.**

The major goals set in the original project management plan for this phase of work were: (a) preparation of low-density $CO_2$ foamed samples in laboratory pressure vessel and optimizing pressure vessel foaming conditions to be used for pilot/factory production, (b) reducing foaming pressure by enhancing $CO_2$ solubility and reducing foam density to below 35 kg/m$^3$, (c) addition of radiation blockers to increase foam R value from R-4.1/inch to R-5/inch, (d) controlling pore size and morphology to further increase R value towards R-6/inch. Advancements towards these milestones in pressure vessel foaming are summarized.

### Optimization of foam densities

We were able to adjust several different foaming condition parameters to lower the sample density by almost 3 times (from 0.1 gram/cc to 0.035 gram/cc). We were able to adjust several different foaming condition parameters to produce foams with densities as low as 33 kg/m$^3$. The R value normally increases with density reduction until radiation heat transfer became dominant. Thus, additional density reduction was attempted with the increased addition of radiation blockers. The photographs below in Figure 4 and Figure 5 are earlier examples of two large foam (samples (density of 40 and 50 kg/m$^3$ respectively) made by the new pressure vessel.

## $CO_2$ Solubility Enhancement – Feasibility has been demonstrated

One major technical barrier of replacing the current HFC blowing agents with $CO_2$ has been the anticipated substantially higher processing pressure at the die exit. This is a necessary practice for compensating for the lower $CO_2$ gas solubility by holding the gas mixture at a higher equilibrium pressure (Henry's law) and preventing premature foaming within the extruder die. We proposed the use of solubility enhancement additives to lower the pressure of a foaming process. The low density foam was produced from polystyrene compounded with an organoclay made with amino-undecanoic acid (AUA). It is hypothesized that the AUA acts to increase solubility of $CO_2$. The samples with solubility enhancement achieved the low density with significantly lower soaking pressure (100 bar) instead of 135 bar without solubility enhancement). This was a promising development as we may be able to apply material technology to ease the processing constraint of switching from HFCs to $CO_2$, which was the primary objective of this project.

**Figure 4. ISTN3-9. Foamed at 121°C, 110 bar. Foam diameter 165mm.**

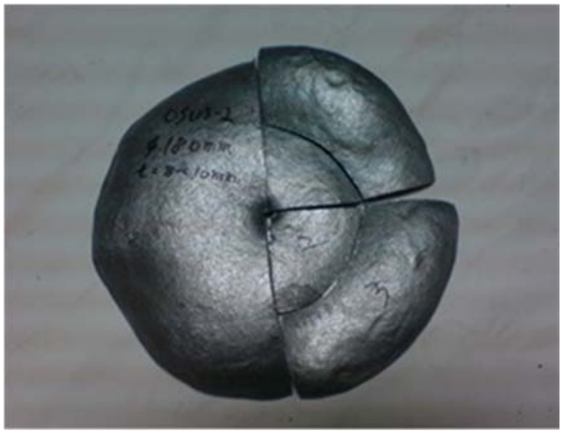

**Figure 5. ISTN4-2B. Foamed at 121°C 110 bar. Foam diameter 120mm.**

## Secondary nanostructure and oblate pore structure by use of polymer blends

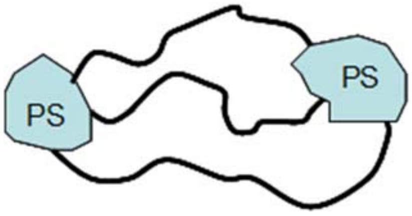

**Figure 6. SEBS.**

It is hypothesized that addition of elastic component could improve the foaming density as well as allowing side-chain modification for secondary nanostructure to be tested in larger-scale foaming experiments. SEBS (polystyrene-*block*-poly(ethylene-*co*-butylene)-*block*-polystyrene block copolymer) is a tri-block copolymer with the elastomeric hydrogenated ethylene/ butylene segment (EB) sandwiched between two end polystyrene blocks (as illustrated). Through a collaboration with Taiwan Synthetic Rubber Company (TSRC) we explored the blending of SBS and SEBS into the PS resin for making a new generation of thermal insulation foams by creating an intertwined nanostructure. The two styrene-blocks would most likely be anchored within the main polymer phase (PS) of the cellular wall, while the EB blocks, with appropriate side-chain modifications, could remain in air pocket as basis for forming the intertwined secondary structure. Our concept of incorporating this copolymer was intended for accomplishing two objectives: (a) Reducing the total foam density by increasing the porosity of the non-load-bearing EB block, and (b) Separating the EB segments with peroxide or other curing agents to create the secondary intertwined nanostructure.

The addition of only 10% of SEBS thermoplastic elastomer into the viscous PS resin can make foaming more difficult because of the drastically different relaxation behaviors among respective viscous (PS) and viscoelastic (SEBS) phases. The substantial density increase (from 40 kg/m$^3$ to 258 kg/m$^3$) of the first few samples foamed at conditions virtually identical to previous experiments had manifested the challenge of including such elastomer in foaming polystyrene. However, with the adjustment of the timing of pressure quenching (from 1 second to 3 seconds) we were able to produce PS+SEBS samples not only without any blisters and blow holes, but also achieving a low density of 33 kg/m$^3$ (photographs shown below).

**Figure 7. ISTN6-7A: Foaming T 123°C, Density 258 kg/m$^3$**

**Figure 8. ISTN6-7B: Foaming T 123°C, Slower (3 sec) gas discharge, Density 33kg/m$^3$**

We believe these experiments had achieved a major innovation of upgrading polystyrene building insulation with the addition of SEBS and subsequently filed a patent. We had conducted more experiments both in the pressure vessel as well as on the pilot line and in factory trials that had further demonstrated the benefits of this new technology.

IR reflective aluminum flakes

From our theoretical modeling work and previous experimental data, we believe the most effective approach of blocking radiation heat transfer is by adding reflective metal flakes. However, previous experiments also revealed difficulties of processing aluminum flakes as well as its adverse effects on foam densities. By selecting new aluminum flake additives we were able to compound as much as 3.75% of aluminum flakes within the resin and successfully made low-density foams embedded with aluminum flakes. The photograph shown in Figure 9 is a sample containing aluminum flakes and showing their characteristic shiny, reflective grey color even at a low weight fraction. The foam density was still higher than samples made without aluminum flake additives. In order to achieve the R-5/inch value we targeted, the density needed to be reduced below 40 kg/m$^3$ which was later achieved in the pressure vessel experiments (shown below) and verified in full scale factory trials. Reflective radiation blockers were successfully incorporated into foam samples and the density was lowered to the lowest 0.033 g/cc. We measured thermal conductivity of a few samples and obtained R value of R-4.5~4.8/inch. Based on these results and our modeling calculation, we designed the recipes containing SEBS and Al flakes for factory manufacturing trials with samples at production reaching R-5/inch. While lowering density is most effective in increasing R value, it reaches a limit when radiation heat transfer becomes appreciable (sometimes 20 % of the total heat transfer). Thus, density reduction must be accompanied by addition of radiation (IR) blockers. One of the most significant progresses in the vessel experiments was that we produced a sample with Aluminum (Al) flakes and also with the lowest density as shown in Figure 10.

**Figure 9. ISTN3-8 with 1.9% Al additive. Foam density = 33 kg/m3 Aged R value/in = 4.55.**

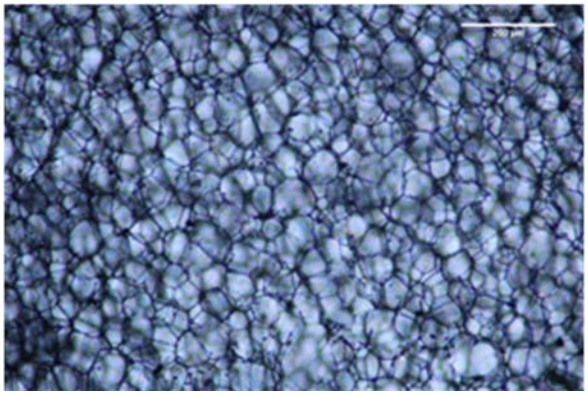

**Figure 10. ISTN3-8 light transmission photomicrograph. Mean cell diameter 45µm ±10µm.**

<u>Homogeneous nucleation</u>

We already demonstrated the feasibility of initiating a homogeneous nucleation during foaming experiments performed in the pressure vessel. We foamed pristine PS resin without any additives to eliminate the heterogeneous nucleation often occurring within purposely added porous additives such as talc. The resin can be foamed to low density (42 kg/m$^3$) which indicated the existence of homogeneous nucleation. However, judging from the cell size (90 ± 10 µm), cell coalescence effects or homogeneous nucleation had not reached the desired level. The key to making nanopore super insulation by foaming is to reinvent and control homogeneous nucleation. Because of the extremely high porosity (97%) required by an insulation foam, the homogeneously created nuclei must appear in very high population density as well. The average cell diameter of the pressure vessel foams (96% porosity) was in the range of 100 micron, 10 times larger than the targeted milestone value (10 micron). We can achieve such a reduction in pore size by lowering the dynamical interfacial tension of the $CO_2$ bubbles. We had already developed a proprietary resin modification idea capable of creating low interfacial energy center for bubble nucleation.

## B. <u>Pilot Extrusion Phase Experiments and Results</u>

In order to expedite the scale-up process for 100% $CO_2$ foaming, we concentrated on creating foam insulation material at the pilot and small-production scale utilizing external extrusion equipment. Several external facilities were evaluated and based upon the contract cost, project details and capability, we initially selected Polymer Processing Institute, Newark NJ ("PPI) for compounding and foaming experiments and subsequently LTL Color Compounders LLC ("LTL") for compounding and MuCell Extrusion LLC (Woburn, MA) to run pilot-scale foaming experiments.

### Pilot Extrusion Experimental Design and Focuses

A major mission of this project was to commercialize 100% $CO_2$ foaming technology for building insulation production in order to completely eliminate the use of HFCs in foam production. Thus, every technology advancement achieved by the project in laboratory must be quickly scaled up to the pilot level and then eventually to the manufacturing scale. Our focuses of pilot experiments are (a) lowering foam density (30-35 kg/m$^3$), (b) making R-5/inch insulation foam with 100% $CO_2$ blowing agent, (c) creating oriented oblate pore structure to further enhance R-value, (d) modifying die design to produce thicker insulation foam with 100% $CO_2$.

We had previously produced in pressure vessel foam samples loaded with radiation blockers and with insulation value approaching R-5/inch. The objective of this element of work was to demonstrate such improvement capability by an actual extrusion production process. Such foaming experiments were successfully scaled up to pilot extrusion level at the facility of PPI and at MuCell Extrusion LLC (Woburn, MA).

The objective of the work at PPI was to compound various PS formulations using Leistritz twin screw extruder and study the feasibility of producing low density foam rods with small cell size using various PS formulations in a tandem extrusion system utilizing 100% CO2 as the blowing agent. A 34 mm Leistritz twin screw extruder was used for compounding the polymer/additive mixtures at 15kg/hr.

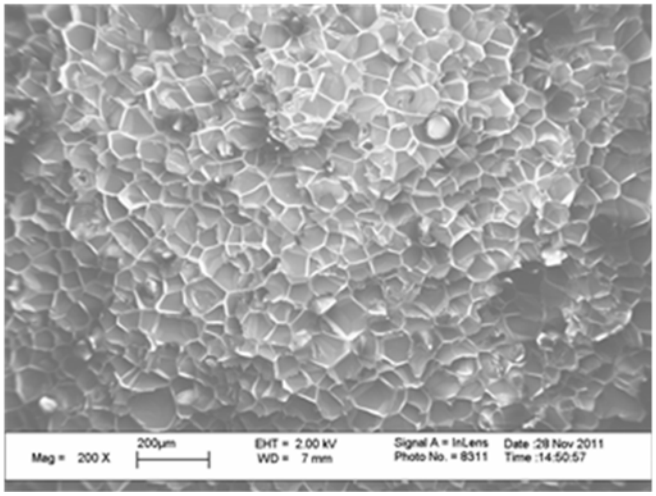

**Figure 11. Scanning Electron Micrograph of foamed sample #11-9-11-11.**

A tandem extrusion system, consisting of a 34 mm diameter co-rotating twin screw extruder (mixing extruder) feeding a 40 mm diameter single screw extruder (cooling extruder), was used for the production of the foam samples. Polymer pellets were fed into the hopper of the twin-screw extruder through a solid metering feeder. The blowing agent was injected in the twin-screw extruder through a positive displacement pump (dual piston HPLC pump) at 20 L/D of the extruder, after a complete melting of the material was achieved. The screws of the twin-screw extruder were specially configured to ensure good mixing of polymer and blowing agent. The barrel and the die temperatures of the single screw (cooling) extruder were controlled using four separate oil heaters to achieve proper cooling and temperature control. A 4 mm rod die was attached at the end of the cooling extruder. Polymer throughput was approximately 2.5 kg/hr. The density ranges achieved with all formulations (**Table 7**) were around 58-70 kg/m$^3$, except for sample #11-9-11-11 (with IR blocking additive). This sample had a higher density compared to other foamed products but its SEM image (**Figure 11**) showed very small cell size and very uniform cell size distribution.

| Sample # | Resin | Die Pressure psi | Density (kg/m$^3$) | Cell size range (µm) |
|---|---|---|---|---|
| 11-8-11-5 | PS1700+ 2.3% Clay-1 | 1500 -1600 | 66 | 100-160 |
| 11-9-11-9 | PS1600 +2.6% Clay-2 | 1500-1600 | 78 | 80-180 |
| 11-9-11-6 | PS1600 + 9% Kraton FG-1901 + 2.5% Clay-1 | 1800-1900 | 58 | N.A. |
| 11-9-11-11 | PS1700+ 2.3% Clay-1+ 2% Al | 1100-1300 (fluctuations) | 95 | 30-50 |

**Table 7. Density and cell size of selected samples foamed at PPI.**

The conclusion from the foaming tests at PPI was that larger pilot extruder equipped with slot die design and accurate $CO_2$ metering was necessary to produce lower density foam and also in a shape useful for thermal property measurements.

The single screw tandem line at MuCell was equipped with a slot-die designed to generate 2500 psi pressure at the head. The 2½ inch diameter extruders were operated at feed rate of approximately 45 kg/hr. Extruder parameters (screw speed, temperature zones, carbon dioxide gas flow) were adjusted to optimize the foam board density. Three extrusion experiments were conducted testing our material modification and processing improvements. Trials were conducted with virgin resin and with two levels of the aluminum radiation blocker pigment. For the first trial, no nucleating agents were added since the extrusion conditions are favorable for the homogeneous nucleation of the carbon dioxide from the polymer melt. A photograph of the virgin resin foamed board exiting the die is shown in Figure 12. The densities of the trial run samples were in the range of 35 - 40 kg/m$^3$.

The thermal conductivity measurements of these samples showed improvements with the addition of radiation blockers, but not as much as those achieved by samples foamed in a pressure vessel. The fact that the degree of improvements was not directly in proportion to the amount of embedded radiation blocker leads to the conclusion that the dispersion of radiation blocker in extrusion runs might not be adequate at higher levels of additive. In the second pilot run and later factory trials we compounded the radiation blockers into a master batch prior to foam extrusion to facilitate its dispersion during the extrusion process which indeed improved the R-value to our projected level.

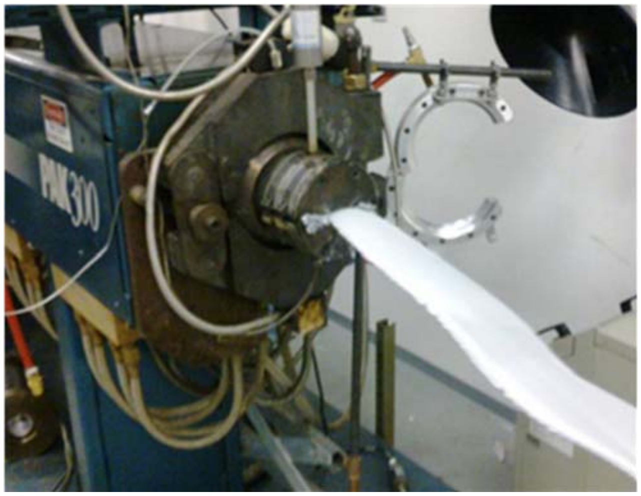

**Figure 12. CO2 foaming of polystyrene with a slot-die at Mucell Extrusion LLC.**

## Thermal Conductivity Measurements

Testing was carried out using the 15cm x 10cm ASTM C1114 fixture, foam samples were cut to 6 – 7mm thickness using a hot-wire device. The relative error in the thickness was generally acceptable (0.5 – 1.25%). Two pieces of foam per side were used because the useable width of the extruded boards was 6 – 8cm.

Pilot extrusion of R-5/inch foam with 100% $CO_2$ blowing agent

| Trial M2 - | PS1600 | SEBS-MA | Clay [10A] | Al Pigment | Foam Density ρ, kg/m3 | λ (23°C) W/(mK) x $10^{-3}$ | R/in |
|---|---|---|---|---|---|---|---|
| 1 | 100% | 0% | 0% | 0% | 38.1 | | |
| 2 | 88.0% | 9.0% | 3.0% | 0.0% | 40.5 | 33.0 | 4.37 |
| 3 | 85.2% | 8.9% | 3.0% | 3.0% | 45.0 | | |
| **4** | **91.0%** | **5.4%** | **1.8%** | **1.8%** | **41.0** | **31.3** | **4.61** |
| 5 | 85.2% | 8.9% | 3.0% | 3.0% | 45.9 | 32.6 | 4.42 |
| 6 | 80.2% | 11.9% | 4.0% | 3.9% | 39.7 | 32.3 | 4.46 |

**Table 8. Select formulation and results of density and thermal conductivity measurements from MuCell**

**trial.**

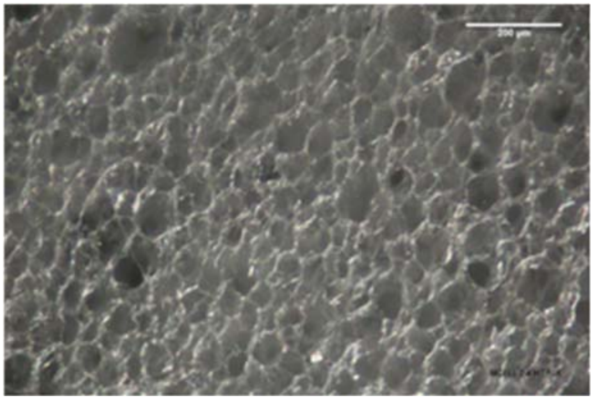

**Figure 13. Reflected light photomicrograph of M2-4 foam. Mean cell diameter 43µm ± 15µm.**

The highest R-value achieved in pilot extrusion (trial M2-4 at R-4.61/inch). A photomicrograph of sliced section of this foam is shown in Figure 13. Our modeling calculations indicated that we could increase the R-value to R-5/inch by lowering the foam density to 30 $kg/m^3$. The processing parameter control in the pilot extruder was not as good as in a full production line and hence it was not possible to lower the density further. Nevertheless, the pilot extrusion experiments had generated sufficient data and information that led to the successful full production line trials later.

## Creating oriented oblate pores by restricting expansion ratios

We had designed a device that can be attached to the die of the pilot extruder to restrict the foam expansion after its exiting from die. The following design called for the plates to be installed at the exit of the extruder and clamped down by nuts and bolts to maintain the gap between the plates. The width of the gap between two plates was reduced to limit the expansion in the direction vertical to the machine extrusion direction. Teflon coating was applied to minimize friction resistance between the foam and the plates. We tested this device at Mucell during a third trial. The extruding power of the pilot line was not strong enough to overcome the friction force from the top and bottom plates. (Similar devices had been used in a full production line which had a much higher throughput than the pilot extruder we were using.) We were able to produce restricted-expansion samples by adjusting the gap of the belt puller. However, the first set of results was not conclusive in geometry and orientation. Restricting the height of the foam using the belt puller also consistently increased the foam density.

The foam board was cut in three orthogonal directions with x-y plane sliced parallel to machine direction, x-z plane sliced parallel to cross machine (width) of foam and y-z plane sliced parallel to parallel to height of foam. Restricting the foam as in exits the die does not significantly alter the cell size and there was no significant orientation in the cell morphology as shown in the figures below.

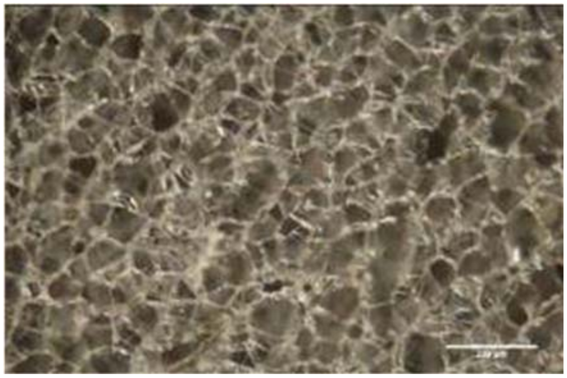

**Figure 14. Optical micrograph of foam M3-3 cut in Machine Direction X/Z Plane.**

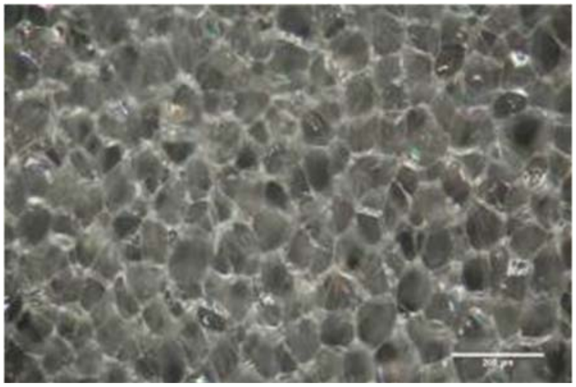

**Figure 15. Optical micrograph of foam 3-3 cut in Cross-Machine Y/Z Plane.**

## Pilot Extrusion of Foam with SEBS

We have successfully incorporated SEBS into material batches and produced good foams in pilot extrusion experiments. Foaming SEBS in a pressure vessel was considerably more difficult than foaming PS. The cell structure and foam quality of pilot extruded foams were generally similar to samples from the pressure vessel. During these pilot experiments, we did discover another important advantage of using SEBS. SEBS is an elastomer and could improve the toughness of the foam product and the stability of the foaming process. Additionally, we could further use SEBS's elasticity to expand the foam through externally induced tension force. This idea had been included in the new design of the die. We filed a provisional patent based on new design of the die and the use of tension force to increase expansion ratio in machine direction (by pulling).

## New Design of Die to Allow Thicker Board Production

One primary reason that foam producers have been doubtful about the 100% $CO_2$ foaming technology to this point is the limitation in thickness range of their $CO_2$ blown foams. The $CO_2$

foaming production has generally required a much higher die pressure in order to dissolve sufficient gas to accomplish a low density. As a result, the die opening must be kept very small, preventing the production of thicker insulation board (above ½ inch). ISTN had developed a proprietary die design that could maintain a high die pressure without sacrificing the thickness of the foam board. Additionally, this new design, because of the capability of maintaining a high die pressure, allows additional post-die attachment to control the expansion ratio in the vertical direction. Such an integrated design could help create and orient oblate pore structure right after the die exit. **A provisional patent application had been filed based on these experimental results**.

## C. Factory Trial Run Results

### Results of Factory Foaming Trial

We carried out a full-scale foam production trial at a plant in Shanghai China and basic compositions of the master batches used are given in the table below:

| **Batch number** | **MB-1** | **MB-2** | **MB-3TW** | **MB-3US** | **MB-4** |
|---|---|---|---|---|---|
| **Ingredient** | | | | | |
| Polystyrene resin | 64% | 67% | 85% | 85% | 80% |
| SEBS polymer | 36% | 27% | | | |
| Clay | | 6% | 15% | 15% | |
| Aluminum MB | | | | | 20% |

**Table 9. Shanghai trial masterbatch compositions.**

During the three day factory trial, the tandem single-screw extruder was operated at approximately 430 kg/h and the pressure at the exit die was 65 – 80 bar. (This head pressure is too low to reduce pore size and should be increased with using new die design in future factory work.) Full-size foam boards with thickness 35-40 mm and widths up to 75 cm were produced. By use of a blend of $CO_2$ (up to 60% w/w) and ethanol as the low GWP physical foaming agent, it was possible to obtain well-formed XPS boards with low density (29 – 33 $kg/m^3$ ) for a majority of the compositions by extruder die fine-tuning and optimizing the melt temperature especially for recipes containing aluminum additives. For thermal conductivity measurement, the extruded boards were cut into 30cm square pieces and measured using a guard hot-plate instrument and also additional measurements were made on aged foams at ORNL (Building Envelope Research) using a heat flow instrument. Selected compositions and results of measurements carried out on the foam boards are given in **Table 10**.

| Trial | Density (kg/m$^3$) | Avg. Cell Size (µm) | R-value/inch, Age = 10d | R-value/inch, Age = 48d or 58d* |
|---|---|---|---|---|
| 10 | 29.9 | 169 | | |
| 12 | 30.3 | | | |
| 17 | 33.1 | | | |
| 18 | 32.5 | 135 | 4.85 | 4.47 |
| 19 | 33.0 | 150 | | |
| 21 | 30.5 | | | |
| H0 | 32.9 | 174 | 4.02 | 4.11 |
| 22 | 29.7 | 436 | 3.78 | 3.71 |
| 23 | 29.3 | 463 | | |
| 24 | 30.4 | 279 | | |
| 25 | 30.8 | 192 | 3.82 | 4.04 |
| 27 | 30.4 | 266 | | 3.89* |
| 28 | 30.4 | 223 | | 3.87* |
| 30 | 32.6 | 156 | 4.95 | 4.55, 4.49* |
| 31 | 32.6 | 116 | 5.17 | 4.68, 4.53* |

**Table 10. Selected factory trial results.** Measurement Conducted at ORNL using ASTM C518 Test Method (Mean Temperature 23.9˚C).

Increasing the puller speed stretch the foam as it emerged from the die to magnify orientation of the cells was also attempted for trial #19 - 21. It was possible to do this while still producing a well-formed board. Optical micrographs of foams sliced in the transverse and machine directions are shown in which showed anisotropic pore structure.

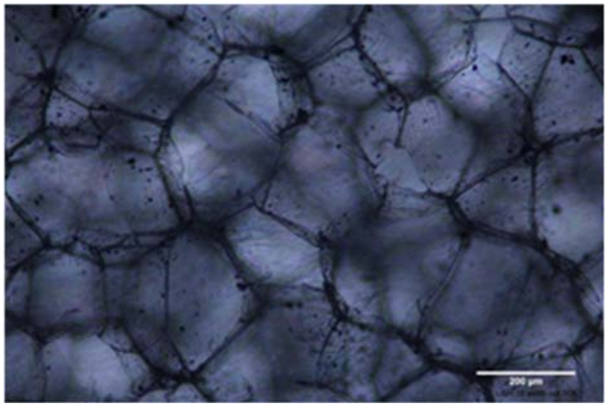

**Figure 16. Optical Photomicrograph of Polystyrene (SH-18) Foam Sliced in Cross-Machine Y/Z Plane.**

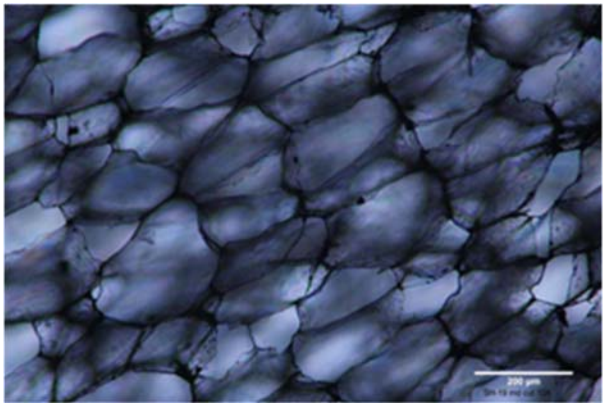

**Figure 17. Optical Photomicrograph of Polystyrene (SH-18) Foam Sliced in the Machine Direction X/Z Plane.**

## Polymer Blend A Foaming and Aging Studies

We acquired for thermal conductivity measurement several 30cm x 30cm x 5.6cm foamed Polymer Blend A boards from a well-known, large European manufacturer of polymer foams. These foams were expanded with a hydrocarbon blowing agent (with low GWP) to a density of 60 kg/m$^3$. We submitted the Polymer Blend A foams to the Building Envelope Research division of ORNL for initial thermal conductivity measurement to be followed by an accelerated aging test. The measured value using ASTN C518 test is 27.7 x $10^{-3}$ W/(m·K) or R/in value of 5.2. Previous inhouse aging tests done by the European company had demonstrated excellent aging performance over PS and PU insulation.

# 5. Conclusions

## (A) Cost-effective HFC-free building insulation with enhanced R/inch performance

The major goal of this project was to produce enhanced building thermal insulation with cost competitive to common building insulation. Any improvement in R/inch performance must be judged by the cost increase on per R basis. Therefore, any advancement in insulation performance at laboratory must be further demonstrated at the full factory production trials in order to assess the final cost of the new insulation products.

Present building insulations have exceptionally high, i.e. ~ 97% porosity and thus, extremely low material cost. The factory production of an advanced building insulation is extraordinarily challenging as processing the high porosity (by foaming) must not only be within the cost limitation of conventional foam extrusion standard, but also be precisely as high to control the base material cost. For example, a small decrease in porosity from 97 to 96% would amount to 25% material cost increase (foam density increased from 30 $kg/m^3$ to 40 $kg/m^3$) even without losing its insulation performance. This has long been the reason of not having any significant product improvement over the past seven decades.

Another major technical difficulty in running a factory production test is the high throughput of the foam extrusion process, which itself is the reason for minimizing the processing costs of insulation. Any attempt of experimenting a new recipe to improve insulation performance must overcome not only the high porosity extreme hurdle, but also the enormous amount of scrap insulation generated along with tuning production run conditions. We tested our material recipes at a throughput rate of 450 kg resin per hour, which, given the targeted 30 $kg/m^3$ insulation density, generated 120 $m^3$ (~53,000 board-ft.) waste material in one day. Our production collaborator had a recycle system that can partially reclaim the raw material consumed by our three-day trial run experiments. Nevertheless, the logistics of handling the enormous amount of waste, particularly in the initial phase of assessing a new recipe's performances, remains to be one of the biggest challenges in the development of a superior building insulation.

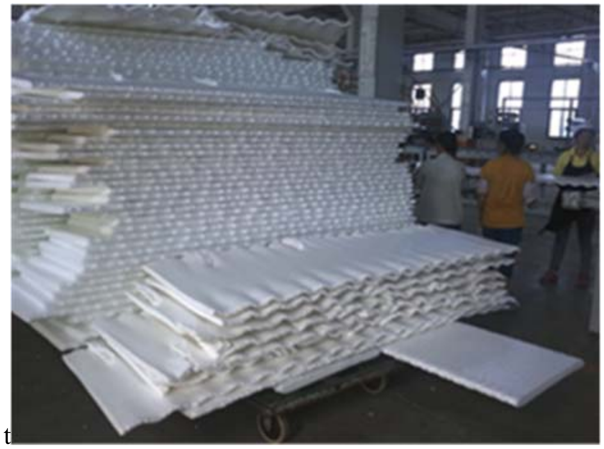

t

**Figure 18. Shanghai trial. Foam product.**

**Figure 19. Shanghai trial. Extrusion line.**

In our three-day factory trial run of several best recipes, which were screened and selected after a series of designed pressure vessel and pilot experiments, we had successfully produced several sets of sample with commercial potential and improved insulation performance. The significant technology advancement of our manufactured products included:

1. The foaming agents were predominately $CO_2$ – achieving the objective of removing the harmful HFC, or HCFC in future building insulations.
2. The product samples were at densities near 30 kg/$m^3$ and thus can be produced in mass production with a cost competitive to present building insulations – achieving our goal of increasing insulation value with justifiable cost on per R basis.
3. Several sets of samples had insulation value in the range of R-5~5.5/inch with implementing our technologies of IR blocking additive and oblate pore structure control – achieving R-5/inch insulation produced at the manufacturing scale and with affordable costs.

Part of the successes in insulation enhancement was attributed to the compounding of aluminum flakes into a master batch prior to foam extrusion which may slightly increase the processing cost in future with justifiable performance enhancement. The oblate pore structure was created by a pulling force applied to insulation boards after their exit from the extruder die. The enhancement in insulation performance from this treatment did show a regression due the dimensional change caused by the elasticity of the SEBS additive. From this trial run we further developed a new die design which could lead to oblate pore structure without the concern of thermal relaxation after production. The concept was filed for a patent and illustrated by the diagrams below.

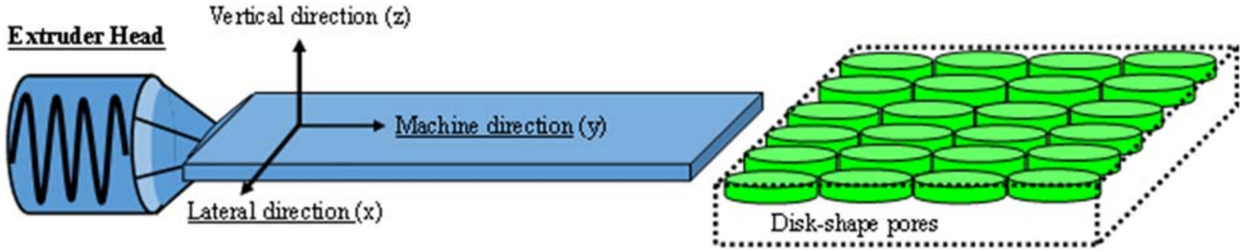

**Figure 20. Extrusion process concept design.**

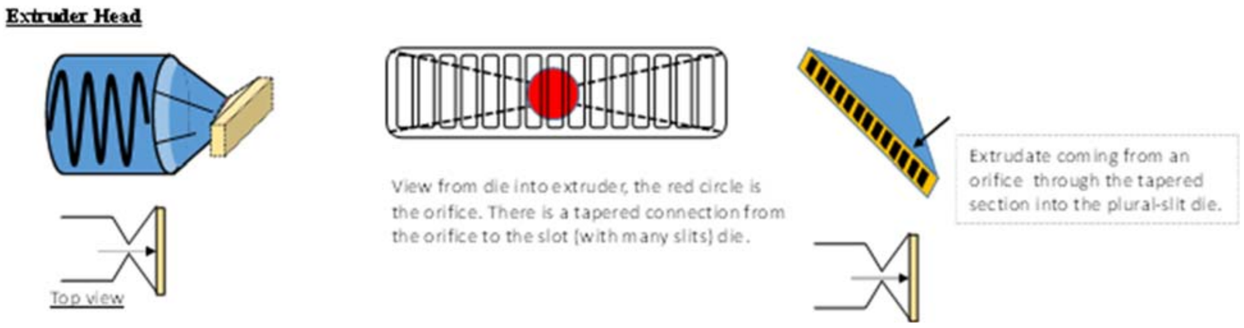

View from die into extruder, the red circle is the orifice. There is a tapered connection from the orifice to the slot (with many slits) die.

Extrudate coming from an orifice through the tapered section into the plural-slit die.

**Figure 21. Extruder die design.**

The die modification would shape oblate pore structure nearer to the die exit and thus lower the likelihood of contraction after foam curing and preserve the higher insulation value resulted from the oblate pore structure.

### (B) New Building Insulation of R-6/inch Performance

We have been closely examining Polymer Blend A foaming technology since early 2010. Based on our modeling calculation along with some preliminary data analysis, we are convinced that Polymer Blend A foam insulation could replace incumbent polystyrene insulation in future building material market. PS has been used as building insulation for almost 70 years and its insulation value can hardly be improved beyond R-5/inch even with the inclusion of harmful

HCFCs. Compared to PS insulation, Polymer Blend A building insulation would have the following distinctive advantages:

(a) Polymer Blend A is an engineering plastic and a stronger structural material than PS

(b) Polymer Blend A insulation can be made of plastic recyclable from bottles of water and drinks

(c) Polymer Blend A contains functional groups that are as good a radiation absorber as those in polyurethane (PU) and polyisocyanurate (PIU) and thus could raise R value above PS insulation to those achievable by PU and PIU insulations (R-6~7/inch)

(d) Polymer Blend A can be blown with pentane gas which has similar insulation enhancement power as HCFC, but with much reduced global warming power

(e) Polymer Blend A is the best vapor barrier and could hold insulation-enhancement blowing gas much longer than PS insulation, or any other polymers currently available in insulation market

We always believed the two major challenges of developing a new generation of Polymer Blend A building insulation had been (1) Foaming Polymer Blend A to a very low density (i.e. below 40 $kg/m^3$), and (b) Achieving same performance comparable to PS insulation in real fire tests. Polymer Blend A resin is denser than PS (specific gravity of 1.3 versus 1 for PS) and requires a higher blowing ratio (i.e. higher porosity) in order to compete with PS on the material cost basis. Secondly, Polymer Blend A foam is predominantly blown with pentane and could retain pentane for a very long time, which would compromise its resistance to fire. The technical progress achieved by our project on PS building insulation, lowering foam density and with 100% $CO_2$ gas foaming, could help resolve those two challenges and greatly contribute to the development of future Polymer Blend A building insulation product. If successfully made at production level, this could be the fastest way of raising the R-value of building insulation from present R-5/inch to above R-6/inch or even higher.

We have been collaborating with a leading European insulation foam company on the development of Polymer Blend A foam for a new generation of building insulation. Polymer Blend A is an engineering plastic that has an outstanding mechanical strength particularly suitable for building insulation application. In addition, the excess Polymer Blend A wastes generated by the bottling and optical industries globally can be turned into a valuable raw material source for an energy-saving insulation product.

Based on extensive R&D work supported by this grant we have concluded that the technology and market barriers against super insulation products are how to produce them cost-effectively so that the cost-per-R-value is competitive to existing insulation products in the same market. Nanopore insulations can easily reach R/inch value of 8 to 10 but the cost per inch thickness is several times higher than the PS insulation, and thus, could only be applied in a few niche markets situations as specialty insulations.

Polymer Blend A insulation's most appreciable difference from polystyrene is the potential upgrading of insulation value beyond R-6/inch due to its stronger radiation absorption power and gas retention capability. Consequently, Polymer Blend A could become the best bulk polymer for a future generation of building insulations. With implementing additional additives and pore morphology control technologies developed by this project, future building insulations could be upgraded to the range of a super thermal insulation (R-value in the range of 8-10 per inch).

We have discussed with our European collaborator the possibility of a co-development and cross-licensing partnership that would allow us to apply ISTN foaming technology to further improve the insulation value and the fire resistance rating of future Polymer Blend A insulation. The collaborating company already produce a number of foams based on Polymer Blend A with a density of 80 $kg/m^3$, and were able to produce lower density Polymer Blend A foam insulation (~40 $kg/m^3$) at a pilot scale extrusion line.

The company was interested in ISTN technologies of (a) $CO_2$ gas foaming to reduce flammability of current blowing gas of cyclopentane, (b) SEBS-Ma additive and nucleation package to successfully scale-up density lowering technology to full production scale, (c) New die design to elevate head pressure of extrusion line and consequently create finer cell structure to further increase the R/inch value of Polymer Blend A insulation. The following chart is based on preliminary data and calculation that definitely demonstrates the value of our proposed technology improvement and the potential of Polymer Blend A to become the next generation of thermal insulation.

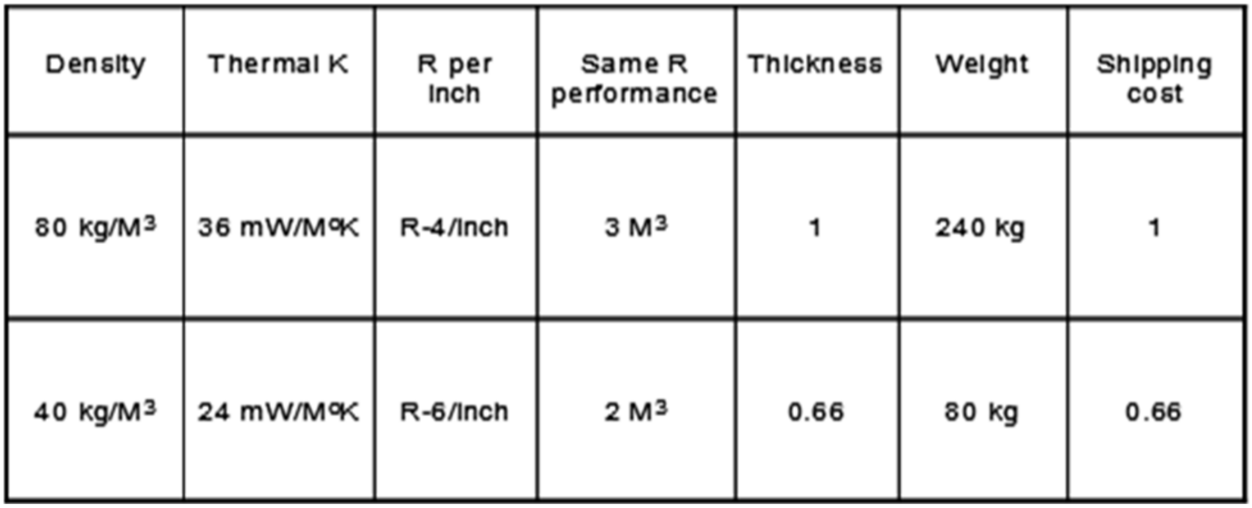

| Density | Thermal K | R per inch | Same R performance | Thickness | Weight | Shipping cost |
|---|---|---|---|---|---|---|
| 80 $kg/M^3$ | 36 mW/M°K | R-4/inch | 3 $M^3$ | 1 | 240 kg | 1 |
| 40 $kg/M^3$ | 24 mW/M°K | R-6/inch | 2 $M^3$ | 0.66 | 80 kg | 0.66 |

**Table 11. Polymer Blend A density optimization.**

The above table clearly confirmed the value addition of our foaming and additive technologies to the Polymer Blend A building insulation. Successful implication of our technologies at production level could help increase R value, reduce application thickness, material costs (by three folds), and even the shipping cost by 30%. This illustrated our point of increasing performance/cost ratio to commercialize an advanced building thermal insulation.

We believe with the following modifications of present foaming technology we could commercially produce an advanced building insulation sooner than any other conceivable approach we have been evaluating. Because Polymer Blend A foam insulation already has the advantage over PS insulation in reduced radiation heat transfer, any technology we have originally proposed towards the development of super building insulation can be accomplished much quicker with using Polymer Blend A as the starting base resin for building insulation (or refrigeration insulation). Thus, all the technologies proposed for R-value reduction, such as (a) smaller pore size, (b) oriented oblate pore structure, and (c) secondary nanostructure in original proposal could be immediately applied to foaming Polymer Blend A for producing an advanced building insulation. Additionally, Polymer Blend A, being one of the best polymer barrier to gas permeation, could also be developed into long-lasting vacuum insulation panel to further augment

R/inch value for refrigeration applications.

b.1) **Using SEBS-Ma and clay composite to lower Polymer Blend A density** – We already designed a processing strategy to incorporate molecules that are capable of cross-linking Polymer Blend A during extrusion to increase the melt strength of Polymer Blend A. Furthermore, with incorporation of SEBS-MA we expect to further improve the toughness of the Polymer Blend A foam insulation and also help reduce pore size and density in foaming as demonstrated by our pressure vessel and production experiments accomplished in the project.

b.2) **A new blowing agent package with $CO_2$ to replace cyclopentane** – Using $CO_2$ to replace harmful, flammable gases could also increase the foaming pressure and create finer pore structure. However, in difference to our trial with PS foaming, ethanol cannot be used in Polymer Blend A system due to its degradation effect on the resin. The $CO_2$ solubility enhancement technology developed by this project could be a valuable option for Polymer Blend A foaming.

b.3) **Modifying the die design to lower density and control pore morphology** – The above mentioned provisional patent of creating oblate pore structure could be applied to Polymer Blend A foaming to further lower density and boost insulation performances. We intend to use a die containing several vertical slit openings, instead of a horizontal single slit die, to increase the pressure holding power of the die (shown figure below) and gain more control in both the size and geometry of the pores.

**Figure 22. Extruder die design.**

We expect the new die design to achieve Polymer Blend A foaming with finer cell structure, higher $CO_2$ content, and most importantly lower-density with improved appearance (currently a problem in the pilot extrusion of low-density Polymer Blend A).

b.4) **Injection molding of Polymer Blend A foam for refrigerator insulation** – An additional innovation of the die modification is to apply vacuum and mechanical pulling after the resins melt leaving the die. We can apply this approach to create anisotropic expansion in an injection molding process and create high-R-value Polymer Blend A foam for refrigerator insulations. Our vacuum drawing approach has a major difference from conventional scheme of density reduction by vacuuming because of the addition of SEBS elastomer. The elasticity of SEBS could help maintain a tension within the melt and thereby allow using the tension to further lower nucleation energy barrier and could additionally reduce pore size to a submicron scale.

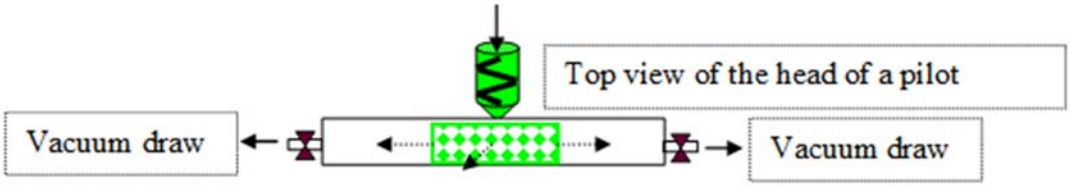

**Figure 23. Creating oblate pore structure by a center-fed injection process.**

### (C) CO2 Foaming of Polymer Blend and Organic-inorganic nanocomposite

In this project we had thoroughly upgraded the foam extrusion process using $CO_2$ predominately as the blowing agent. Along with the development of the next generation of building insulation we successfully invented the high-porosity (low-density) foaming of blends material with recyclable thermoplastic elastomers, for example SEBS, and inorganic nanostructured additive such as silica gel and exfoliated clays.

The new technology, besides of enhancing insulation performance, could become a platform technology to upgrade building as well as many other foam products. For example, the polymer blend foaming can be utilized to produce shoes, furniture, cushioning mats, automobile parts that are environmentally friendly and recyclable. Foaming of polymer-clay composites is also a significant technology advancement that leads to better fire resistance, stronger modulus, and lighter-weight automobile parts.

### (D) Super-Thermal (R-8~10/inch) Insulation with Secondary Nanostructure

This study also provided a feasible route of making super thermal insulations at costs competitive to conventional insulation on per R basis. At present, the barrier against commercialization of nanopore insulation is still its high processing cost. By integrating a nanopore creating process with a conventional foam extrusion process not only could upgrade the present building insulation without a forbidden cost increase, but also allowed creating nanopores with larger pores of an conventional foam during a low-cost foam extrusion process. Such an integration of supercritical drying and foaming (by $CO_2$) into a known low-cost extrusion process should guarantee the processing cost be competitive with conventional insulation material. ISTN is seeking venture capital funding to continue working of scaling-up this process to the pilot and manufacturing levels.

# Appendix

This page left intentionally blank.

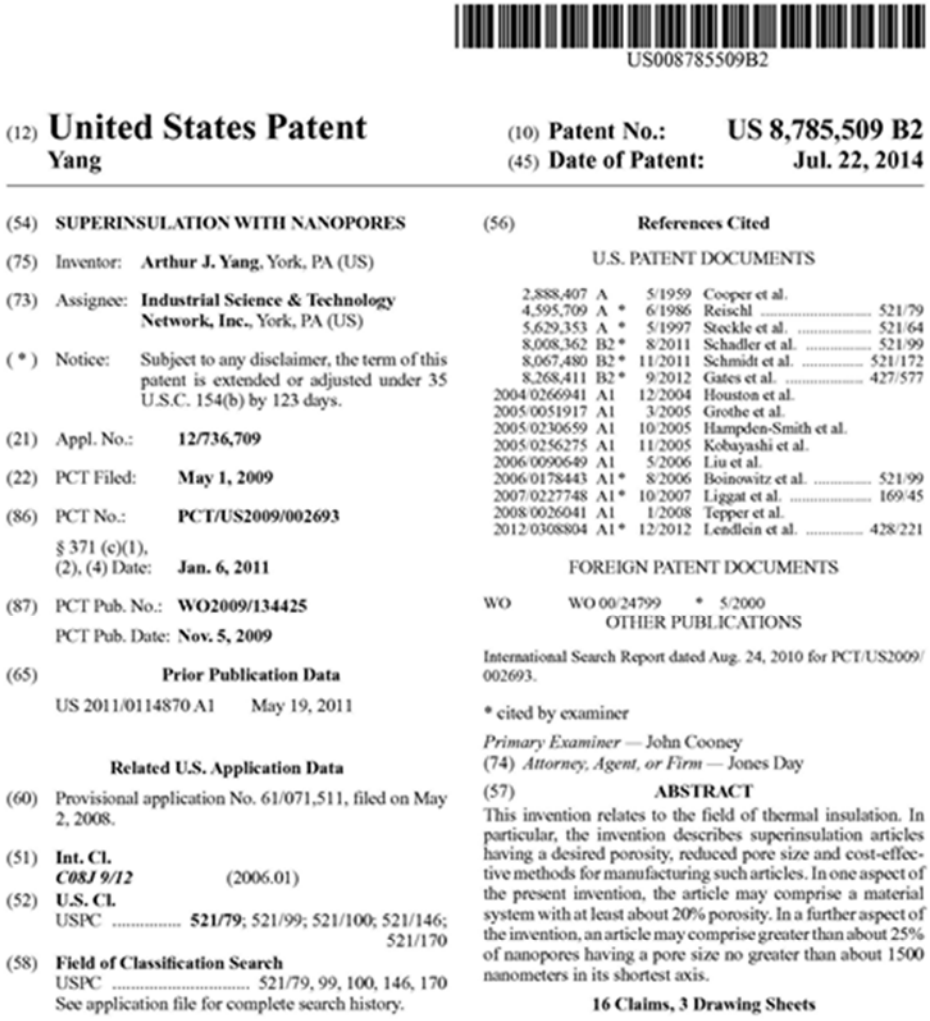

US008785509B2

(12) **United States Patent**
**Yang**

(10) **Patent No.:** **US 8,785,509 B2**
(45) **Date of Patent:** **Jul. 22, 2014**

(54) **SUPERINSULATION WITH NANOPORES**

(75) Inventor: **Arthur J. Yang**, York, PA (US)

(73) Assignee: **Industrial Science & Technology Network, Inc.**, York, PA (US)

( * ) Notice: Subject to any disclaimer, the term of this patent is extended or adjusted under 35 U.S.C. 154(b) by 123 days.

(21) Appl. No.: **12/736,709**

(22) PCT Filed: **May 1, 2009**

(86) PCT No.: **PCT/US2009/002693**
§ 371 (c)(1),
(2), (4) Date: **Jan. 6, 2011**

(87) PCT Pub. No.: **WO2009/134425**
PCT Pub. Date: **Nov. 5, 2009**

(65) **Prior Publication Data**

US 2011/0114870 A1 May 19, 2011

**Related U.S. Application Data**

(60) Provisional application No. 61/071,511, filed on May 2, 2008.

(51) **Int. Cl.**
***C08J 9/12*** (2006.01)

(52) **U.S. Cl.**
USPC ............... **521/79**; 521/99; 521/100; 521/146; 521/170

(58) **Field of Classification Search**
USPC ............................... 521/79, 99, 100, 146, 170
See application file for complete search history.

(56) **References Cited**

U.S. PATENT DOCUMENTS

| | | | | |
|---|---|---|---|---|
| 2,888,407 | A | 5/1959 | Cooper et al. | |
| 4,595,709 | A * | 6/1986 | Reischl | 521/79 |
| 5,629,353 | A * | 5/1997 | Steckle et al. | 521/64 |
| 8,008,362 | B2 * | 8/2011 | Schadler et al. | 521/99 |
| 8,067,480 | B2 * | 11/2011 | Schmidt et al. | 521/172 |
| 8,268,411 | B2 * | 9/2012 | Gates et al. | 427/577 |
| 2004/0266941 | A1 | 12/2004 | Houston et al. | |
| 2005/0051917 | A1 | 3/2005 | Grothe et al. | |
| 2005/0230659 | A1 | 10/2005 | Hampden-Smith et al. | |
| 2005/0256275 | A1 | 11/2005 | Kobayashi et al. | |
| 2006/0090649 | A1 | 5/2006 | Liu et al. | |
| 2006/0178443 | A1 * | 8/2006 | Boinowitz et al. | 521/99 |
| 2007/0227748 | A1 * | 10/2007 | Liggat et al. | 169/45 |
| 2008/0026041 | A1 | 1/2008 | Tepper et al. | |
| 2012/0308804 | A1 * | 12/2012 | Lendlein et al. | 428/221 |

FOREIGN PATENT DOCUMENTS

WO WO 00/24799 * 5/2000

OTHER PUBLICATIONS

International Search Report dated Aug. 24, 2010 for PCT/US2009/002693.

* cited by examiner

*Primary Examiner* — John Cooney
(74) *Attorney, Agent, or Firm* — Jones Day

(57) **ABSTRACT**

This invention relates to the field of thermal insulation. In particular, the invention describes superinsulation articles having a desired porosity, reduced pore size and cost-effective methods for manufacturing such articles. In one aspect of the present invention, the article may comprise a material system with at least about 20% porosity. In a further aspect of the invention, an article may comprise greater than about 25% of nanopores having a pore size no greater than about 1500 nanometers in its shortest axis.

**16 Claims, 3 Drawing Sheets**

**U.S. Patent** **Jul. 22, 2014** **Sheet 1 of 3** **US 8,785,509 B2**

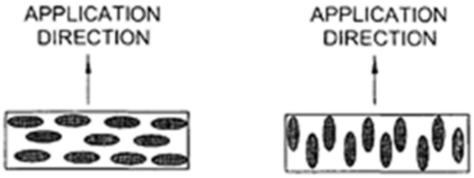

FIG. 1

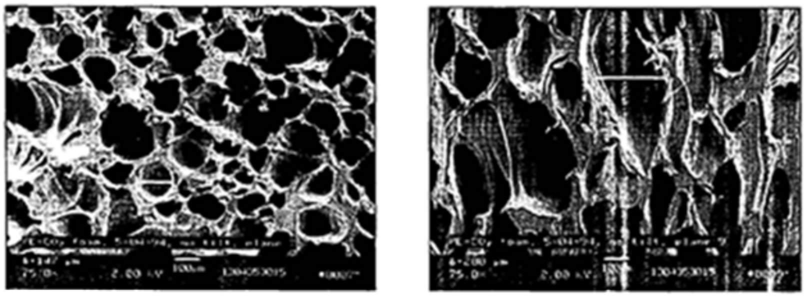

FIG. 2

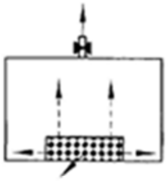

FIG. 3

**U.S. Patent** Jul. 22, 2014 Sheet 2 of 3 US 8,785,509 B2

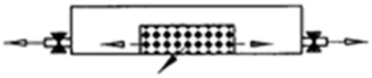

FIG. 4

FIG. 5

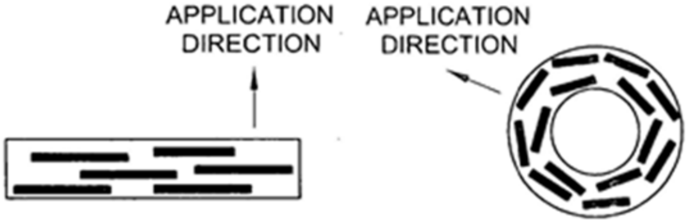

FIG. 6

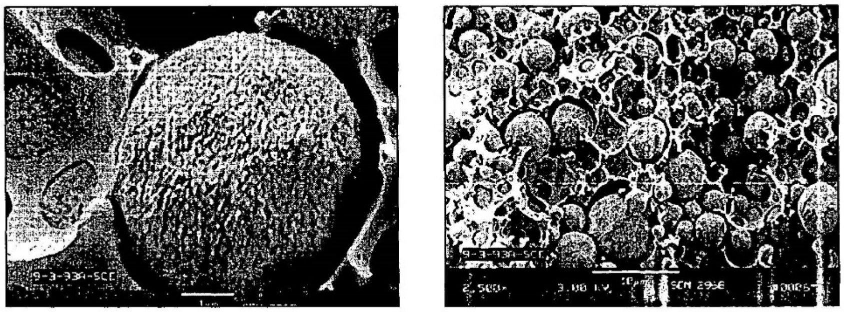

FIG. 7

-continued

| Process Characteristics | Gelation and Drying (Aerogel, Hydrogel) | Direct Gas Foaming (Gas Blown Polymer Foams) |
|---|---|---|
| d. Pore Size Control | 10 nm, needs special processing care to preserve the nanopores | 100-500μ, very difficult to control |
| e. Thermal Conductivity | 20 mW/M°K | 30-35 mW/M°K |

If we can replace the solution drying process and make nanopore insulation by foaming, the cost reductions will be well beyond those needed to make the technology commercially viable. Recently, we had successfully developed the technology of producing low-density (density ~0.03 g/cc) Styrofoam insulation by foaming with 100% $CO_2$. By integrating the two technologies together, we could design a system that utilizes supercritical $CO_2$ to first create and preserve nanometer gas embryos (by a nucleation process), and, then to expand gas bubbles (by a foaming process) for making low-density insulation. Such a system could produce high-porosity foams with extremely small pore sizes. The challenge, of course, remained as how to effectively control the bubbles' size during the rapid foaming process.

A foaming process consisted of rapid generation of numerous gas bubble nuclei, followed by their fast growth during the foam's expansion. We could envision two approaches to control the pore size during such a rapid bubbling process. First, we plan to induce the homogeneous nucleation process (already demonstrated by pressure vessel experiments) in a foam extrusion process to generate extremely small gas embryos, followed by controlling the bubbles' growth. Or, we can use a reactive system, such as the polymerization of styrene or urethane, which secrete out volatile solvent, or co-solvent, during its polymerization and depressurization, to create a spinodal decomposition, followed by controlled expansion of the entrapped volatile fluid phase. Both processes required a low initial interfacial tension, as well as a controlling mechanism to slow down the bubble growths. Either process, if successful in generating fine pores and high porosity, would lead to a breakthrough in producing nanopore insulation because of the tremendous cost savings attributed to the rapid depressurization of supercritical $CO_2$ (or similar volatile fluids). Obviously, such a breakthrough process would be difficult, because it would require orders of magnitude improvement in pore size controls (from ~100 microns to 0.1 micron) comparing to prior foaming arts.

## DESCRIPTION OF THE DRAWINGS

FIG. **1** shows spheroids aligned in-series (left), or in-parallel with the application direction. Left example (in-series) has a higher insulation value than that of right example.

FIG. **2** shows the SEM pictures of the cell structure along two different directions. Through pressurized vessel experiments, foams with anisotropical pore structure have been produced.

FIG. **3** shows the batch depressurization process to create prolate pore structure.

FIG. **4** shows the batch depressurization process to create oblate pore structure.

FIG. **5** shows the use of exfoliated clay platelet molecules to facilitate gas nucleation and asymmetrical expansion, leading to oblate pore structure.

FIG. **6** shows the alignment of exfoliated clays in foam extrusion restricts bubble growth normal to machine direction.

FIG. **7** shows a pair of SEM pictures depicting secondary aerogel fractal structures with two kinds of pores, micron size and nanometer size.

## DETAILED DESCRIPTION OF THE INVENTION

This invention relates to the field of thermal insulation. In particular, the invention describes superinsulation articles having a desired porosity, reduced pore size and cost-effective methods for manufacturing such articles. In one aspect of the present invention, the article may comprise a material system with at least about 20% porosity, for example, 30%, 40%, 50%, 60%, 70%, 80%, preferably at least about 90% porosity, for example, 95%, 96%, 97%, 98%, and 99%. In a further aspect of the invention, an article may comprise greater than about 25%, 50%, 75%, and 90% of nanopores having a pore size no greater than about 1500 nanometers, for example, 1250 nanometers, 1000 nanometers, preferably no greater than about 900 nanometers, 800 nanometers, 750, nanometers, 700 nanometers, 650 nanometers, 600 nanometers, and 550 nanometers, in its shortest axis.

The articles of the present invention, in addition to porosity and a reduced pore size, may also comprise asymmetrical nanopores. In one aspect of the present invention, the articles may comprise greater than about 10% asymmetrical pores, for example, 25%, 40%, and 50%, preferably greater than about 75%, 80%, 90%, and 95%. One aspect of the present invention is an article comprising greater than about 25%, for example, 35%, 50%, preferably greater than about 75%, for example, 80%, 85%, 90%, and 95% oblate or substantially oblate nanopores. Another aspect of the present invention is an article comprising greater than about 25%, for example, 35%, 50%, preferably greater than about 75%, for example, 80%, 85%, 90%, and 95% prolate or substantially prolate nanopores. Yet, another aspect of the present invention may be an article comprising nanopores having an asymmetry unlike oblate or prolate but maintaining a controlled pore dimension in a preferred application directions (e.g. the thermal gradient direction). Furthermore, an article of the present invention may comprise a combination of oblate or substantially oblate, prolate or substantially prolate, and other asymmetrical nanopores.

The articles of the present invention may also comprise nanopores oriented in a preferred direction. In one aspect of the present invention, one or more nanopores are oriented normal to the application direction (i.e. when reference is made herein the orientation of the nanopore is referring to the longest axis of the pore. Therefore, the longest axis of the pore, and the pore orientation, is normal to the application direction. Conversely, the shortest axis is aligned with the application direction) or substantially normal to the application direction. In another aspect of the present invention, one or more nanopores are oriented normal to the thermal gradient direction or substantially oriented normal to the thermal gradient direction. In another aspect of the present invention, one or more nanopores are oriented along the machine direction (i.e. the shortest axis normal to the machine direction) or

substantially along the machine direction. Yet, in one aspect of the present invention, an article may comprise greater than about 25%, for example, 35%, 45%, 55%, preferably greater than 75%, for example 80%, 85%, 90%, and 95%, of nanopores oriented normal to the thermal gradient direction or substantially oriented normal to the thermal gradient direction.

The articles of the present invention may also comprise a secondary nanostructure. Furthermore, the articles of the present invention may comprise a tertiary and/or quaternary nanostructure. In one aspect of the present invention, an article may comprise greater than about 25%, for example, 35%, 45% and 50%, preferably greater than about 75%, 80%, 85%, 90%, and 95%, of nanopores with secondary, tertiary and/or quaternary structure. One aspect of the present invention is an article comprising a secondary nanostructure comprising a surfactant or alternatively any known surface-tension lowering agents or functionally equivalent thereof. A further aspect of the present invention may be an article comprising greater than about 25%, for example, 35%, 45%, and 50%, preferably greater than about 75%, 80%, 85%, 90%, and 95%, of nanopores with a surfactant or known equivalent thereof. Another aspect of the present invention may be a secondary nanostructure comprising an intertwining fractal structure or alternatively a substantially intertwining fractal structure. A further aspect of the present invention may be an article comprising greater than about 25%, for example, 35%, 45%, and 50%, preferably greater than about 75%, 80%, 85%, 90%, and 95%, of nanopores with an intertwining fractal structure and/or substantially intertwining fractal structure. Yet, another aspect of the present invention may be an article comprising greater than 5%, for example, 10%, 20%, 50%, nanopores having one or more secondary, tertiary, and/or quaternary structures.

Furthermore, the articles of the present invention may have a thermal insulation value greater than about 6 R/inch, for example 6.5 R/inch, and 7 R/inch, preferably greater than about 7.5 R/inch, for example 8R/inch, 8.5 R/inch, 9 R/inch, 9.5 R/inch, and 10 R/inch. In another aspect of this invention, the articles of the present invention may have a thermal conductivity value less than about 30 mW/M° K, for example 25 mW/M° K, and 23 mW/M° K, preferably less than about 22 mW/M° K, for example 21 mW/M° K, 20 mW/M° K, and 15 mW/M° K.

The articles of the present invention may be manufactured by creating or generating or substantially creating or generating one or more gas embryos. In one aspect of the present invention, the gas embryos or the known equivalent thereof are created by homogenous nucleation or any other known means of nucleation without preferential nucleation sites. In one aspect of the present invention, an article comprises greater than about 25%, for example, 35%, 50%, preferably greater than about 75%, 80%, 85%, 90%, and 95%, of gas embryos created or generated by such means or the equivalent thereof. In another aspect of the present invention, the gas embryos are created or generated by spinodal decomposition or any known means creating a phase separation throughout the material and not just at the nucleation sites. In one aspect of the present invention, an article comprises greater than about 25%, for example, 35%, 50%, preferably greater than about 75%, 80%, 85%, 90%, and 95%, of gas embryos created or generated by, spinodal decomposition or the equivalent means thereof. Yet, in another aspect of the present invention, a combination of such methods for creating or generating gas embryos may be used.

In a further aspect of the present invention, an article may comprise one or more gas embryos having a size not greater than about 1000 nanometers, for example, 900 nanometers, 800 nanometers, 700 nanometers, 600 nanometers, 550 nanometers, preferably not greater than 500 nanometers, for example, 450 nanometers, 400 nanometers, 350 nanometers, 300 nanometers, 250 nanometers, 200 nanometers, 150 nanometers, 100 nanometers, and 50 nanometers.

In another aspect of the present invention, the gas embryos may be expanded by or substantially expanded by using a foaming process, including any known equivalents means thereof. In one aspect of the present invention, an article comprises greater than about 25%, for example, 35%, 50%, preferably greater than about 75%, for example 80%, 85%, 90%, and 95%, of gas embryos expanded by, or substantially expanded by, batch foaming. In another aspect of the present invention, the gas embryos are expanded by or substantially expanded by a continuous foam extrusion process or an equivalent means thereof. In one aspect of the present invention, an article comprises greater than about 25%, for example, 35%, 50%, preferably greater than about 75%, for example 80%, 85%, 90%, and 95%, of gas embryos expanded by, or substantially expanded by, a continuous foam extrusion process. Yet, in another aspect of the present invention, the gas embryos are expanded by, or substantially expanded by, a combination of such means.

In yet a further aspect of the present invention, the pore size of greater than about 25%, for example, 35%, 50%, preferably greater than about 75%, for example, 80%, 85%, 90%, and 95% gas embryos is controlled by, or substantially controlled by, one or more restriction methods or equivalent restriction means thereof, including any known size controlling methods, affecting one or more of pore morphology, pore orientation, and/or secondary nanostructure aspects of the nanopores. In a further aspect of the present invention, the embedded inert gas may be exchanged by air over time. In one aspect of the present invention, greater than 5% of the inert gas, for example, 10%, 25%, and 40%, preferably greater than 50%, for example, 60%, 70%, 80%, 90% and 95%, may be exchanged by air over time. In another aspect of the present invention, embedded inert gas may be exchanged by air over time, such as greater than 10 days, for example 20 days, 30 days, and 45 days, preferably greater than 60 days, for example, 90 days, 120 days, 180 days, and 360 days. Accordingly, inert gas may include a mixture of the blowing gas (e.g., $CO_2$) and air, for example, at about 10:90, about 50:50, and about 90:10, percent blowing gas to percent air. Furthermore, inert gas may also include 100 percent blowing gas or 100 percent air.

The third generation of thermal insulation is defined as the insulation material composed of air pockets with composition and morphology specially designed to lower the embedded air's thermal conductivity below its ordinary value (i.e. <23 mW/M·° K), resulting in a super insulation of insulation value higher than at least R-7/inch. Prior arts (selected examples shown by above table) demonstrated the feasibility of making insulation with conductivity lower than 23 mW/M·° K when pore sizes were reduced to below the mean free path of air (<100 nm). However, relying completely on pore size reduction to make a super insulation has experienced the tremendous processing challenges when using a supercritical drying process. The inventions disclosed here take a different approach geared towards the cost-effective manufacturing of the third generation of thermal insulation. This new invention contains the following four important components, which collectively could realize the cost-effective production of the third generation of insulation with thermal conductivity much lower than the second generation products:

US 8,785,509 B2

7

(a) Generating homogeneously smaller gas embryos or domains by a homogeneous nucleation, or spinodal decomposition process, using $CO_2$ entrapped as either a blowing, agent or a co-solvent within a polymer system,
(b) Growing asymmetrical (oblate or prolate) pore morphology,
(c) Orienting asymmetrical (oblate or prolate) pores in a preferred direction,
(d) Creating the secondary nanopore structure within air pores.

Prior nanopore structures of super insulation were accomplished by a solution supercritical drying process, which was extremely slow as well as capital intensive. The first innovation in this invention is to use the expansion power of a high-pressure gas embedded in the form of either a solute, or a co-solvent, to create the high porosity required by a super thermal insulation. Furthermore, the gas embryos or domains are created by a homogeneous nucleation, or spinodal decomposition, process in an effort to control the bubbles' growth from their initial births. Previously, gas bubble generation within such a system went through a heterogeneous nucleation process where the initial nuclei provided by the nucleating agents were already much larger than microns. As a result, the pore sizes in prior foams blown using heterogeneous nucleation were already substantially larger than the 100 nanometer required by super insulation.

Early models revealed that the gas thermal conductivity would not be reduced significantly unless the pore size was reduced below a threshold value between 1 and 0.1 micron. The simultaneous requirements of a high porosity (over 95%) and extremely small pore sizes were the main reasons that no foaming processes were successful in producing such a super insulation. After all, the task of increasing thermal insulation value of foams two and a half times higher, from the current R-4/inch to R-7~10/inch is extremely ambitious and, thus, inherently difficult.

The present invention incorporates three additional innovations (b, c, and d listed above) in addition to pore size reduction which are all capable of further increasing the insulation value of a porous substrate. These three options could each individually be utilized to improve insulation value of a current foam product. Collectively, they could be engineered, along with using pore size reduction, to accomplish the required technology jump to that of a super insulation through incremental technology improvements.

One unique aspect of the invention is the recognition and the design to utilize the directional characteristics of a transport property such as the thermal conductivity. For a composite of polymer and air pores, the spatial geometry and orientation of the pores could be utilized to improve the insulation value along the heat flow direction (i.e. the direction of the temperature gradient, or, the application direction). Analogous to the spatial arrangements of resistor-in-parallel (highest conductivity), and resistor-in-series (lowest conductivity), we can utilize the orientations of spheroid pores in parallel (long axis in parallel to the heat flow direction), or, in series (long axis normal to the heat flow direction) to optimize, insulation value. Theory indicated that the increase of heat resistance in one direction (application direction) would be at the expenses of the resistances of the two other directions, which are irrelevant to insulation performances. As shown in FIG. **1**, we have specific modeling calculations to corroborate and estimate these geometry and orientation effects.

The ability of using pore geometry and orientation to further complement the effect by pore size reduction provided substantial leverages of making a super thermal insulation. First of all, the difficult task of pore size reduction (to below the mean free path of air) could be limited to just one direction (the application direction), instead of all three directions. In other words, for spheroids oriented in series with the application direction, only their shortest axes need to be controlled below the threshold value. Relaxations of size controls in the other two irrelevant directions allow a much larger volume for each pore, and therefore, much less pore density be created by foaming. Secondly, the effects of geometry and orientation could help reduce thermal conductivity on top of what already achievable by pore size reduction. Moreover, unlike pore size reduction, the aspect ratio of spheroids has no threshold value to pass. The effects of orientation appear once the shape is asymmetrical, and increase with increasing aspect ratios; resulting the possible stepwise increases of, in conjunction to effect of pore size reduction, thermal insulation value from current standard to that of a new generation.

8

The third generation of thermal insulation material comprising and made from any, or a combination of, the following features:

(a) generating homogeneously smaller gas embryos or domains by a homogeneous nucleation or spinodal decomposition process, using primarily $CO_2$, or a similar inert gas, entrapped as either a blowing agent or a co-solvent in a polymer system,
(b) growing asymmetrical (oblate or prolate) pore morphology,
(c) orienting asymmetrical (oblate or prolate) pores with their short axis along the insulation application (i.e. the temperature gradient) direction,
(d) creating the secondary nanopore structure within air pores, which are to be formed by, but not limited to, the surfactant structure incorporated at the pore surface, or an intertwining fractal structure within each pore.

The material system of the third generation of thermal insulation is composed of a polymer, or a blend of polymers, foamed by embedded $CO_2$, or other inert gases, or their mixtures utilizing a homogeneous nucleation process.

The material system of the third generation of thermal insulation is composed of reactive oligomers such as, but not limited to, styrene and urethane, of which the polymerization reaction is utilized to secrete or generate volatile liquid phase such as, but not limited to $CO_2$, by a spinodal decomposition process for the subsequent expansion thorough the fluid evaporation. The volatile fluids of the system are embedded in under a high pressure, entrapped by the polymer(s) by supercooling, or during polymerization, and later released through an triggered foaming process to produce the insulation on demand and on location.

In the third generation of thermal insulation, one or all of the above attributes (a), (b) and (c) are created through a batch depressurization process designed based on principles of restricting expansion in one direction (the application direction) outlined in Examples 1 and 2 and FIGS. **3** and **4** of this invention.

In the third generation of thermal insulation, one or all of the attributes (a), (b) and (c) are created through a foam extrusion process with a die designed based on principles of restricting expansion in one direction (the application direction) outlined by Example 4 (FIG. **6**) of this invention.

The production of the third generation of thermal insulation by these methods use both platelet molecules of the exfoliated clay to restrict expansion in the application direction (see Example 3 and FIG. **5**), and platelet molecules of chemically modified and exfoliated clay to increase the solubility and the nucleation of the blowing gases ($CO_2$ or other inert gas).

The composition of the third generation of thermal insulation contains exfoliated clays as a major component (i.e. weight % equal to or greater than 5%).

The third generation of thermal insulation is comprised of a polymer-clay composite by the batch depressurization method previously described above.

A third generation of thermal insulation is made of a polymer-clay composite by the foam extrusion method previously described above.

The method of producing a third generation of thermal insulation includes the step of where the foam curing (i.e. stabilization) is accomplished by glass transition (such as demonstrated by polystyrene), crystallization (such as demonstrated by Polyethylene), cross-linking (such as demonstrated by rubbers), or polymerization (such as demonstrated by polyurethane).

A method of producing a third generation of thermal insulation which utilizes a composition including one or more of the components described herein, which is prepared by mixing under pressure in an extruder or a reactor, injected into a mold, followed by the batch depressurization method.

A method of producing a third generation of thermal insulation which utilizes a composition including one or more of the components described herein, which is prepared by mixing under pressure in an extruder or a reactor, stabilized by cooling below glass transition temperature of the polymer (to expandable polymer beads), and then injected into a mold, followed by a heat-triggered depressurization method.

The third generation of thermal insulation with the composition, structure and processing described herein which is utilized as building insulation products, refrigerator insulation products, HVAC (Heating, Ventilating and Air-conditioning) and refrigeration insulation products, industrial insulation products, and/or specialty insulation products, such as, but not limited to, aviation, space vehicles and stations, superconducting devices and equipment.

A porous product with the composition, structure and processing described herein, but with less porosity porosity between 20-90%), may also be used as a foam product for, but not limited to, structural support, cushioning, protection, packaging, sports, entertainment, sound insulating, medical devices, and decoration.

## EXAMPLES

One key step to produce finer-cell, high-porosity foams is to initiate gas blowing from a high pressure-drop. The larger the pressures drop, (i.e. deeper super saturation), the easier the induction of homogeneous nucleation. The challenge of foaming from a high pressure-drop is to control the bubble growth after nucleation. The melt temperature, molecular weight, viscoelasticity must be fine tuned for a successful foaming of low-density insulation. We can first simulate such a foaming process in a pressurized vessel and obtain necessary data of material and processing for future extrusion productions. These batch experiments also help demonstrate the working principles and the feasibility of making a super thermal insulation. They can also be scaled up for batch productions of insulation foam.

### Example 1

### Oriented Prolate Pores Reducing the Thermal K by 10-15%

Through pressurized vessel experiments, foams with anisotropical pore structure have been produced. FIG. **2** shows the SEM pictures of the cell structure along two different directions.

The particular sample shown in FIG. **2** was produced in a pressurized vessel with a sudden release of pressure by opening a valve at the top of the vessel. This setup, as shown in FIG. **3**, provided a favorable direction of foam expansion (towards the top of the vessel), thereby creating anisotropic expansion ratios of the foam (higher expansion ratio to the top than to the sides). The difference in expansion ratios led to prolate (needle-like) cell structure shown by the TEM pictures above. The sample density was 0.023 gram/cc. Thermal conductivities measured along two directions (long polar axis and the short equator axes) were 37 and 33 mW/M·° K, respectively. The 12% reduction in thermal conductivity agreed well with our modeling results for the prolate geometry.

For a blowing and extrusion process, pore morphology control might be easier to achieve than the nanopore feature. The improvement in thermal resistance may be short of the dramatic increase achievable by nanopores, but still significant for gaining ground in the market place and contributing towards the goal of making super insulation.

### Example 2

### Oriented Oblate Pores Reducing the Thermal K by 30%

Our modeling results indicated a more significant improvement in insulation for the oblate geometry (short polar axis and long equator axes, i.e. disk-like) cell structure aligned normal to the heat flow direction. The thermal conductivity of a similar density to the above prolate example could be reduced down to 24 mW/M·° K, which would be even lower than the thermal K of current foam containing low thermal K gas such as HCFC. Such (oblate) cell structure could be created by a batch foaming process with restriction of expansion in the polar direction and free expansion in equator's directions as shown in FIG. **4**.

### Example 3

### Using Exfoliated Clay to Facilitate Asymmetrical Pore Formations

While these two innovations lowered the risks of making large number of nanopores by a foaming process, the technical burden is shifted to the control of pores' geometry as well as their orientation during foaming. This invention includes specific material nanotechnology to facilitate the growth and orientation of spheroid pores. One method is the use of a polymer-clay composite with exfoliated clay layers as template for gas bubble formation. Clay molecules, after full exfoliation, have platelet structure with aspect ratio above 1000. By modifying the surface of a clay platelet, homogeneous nucleation can be enhanced within the galleries of neighboring platelet molecules and increases the formation of oblate pores as shown in FIG. **5**. These highly anisotropic plate molecules (aspect ratio from 40 up to 1000) will be oriented under volume exclusion effect, or by the shear force of the extrusion to the preferred direction. The inorganic fillers can also improve the fire and smoke rating of the plastic foam material.

### Example 4

### Producing Orientated Cell Structure in a Foam Extrusion Process

Create and align oblate pores of an insulation with their short axes all along the insulation application direction (i.e.

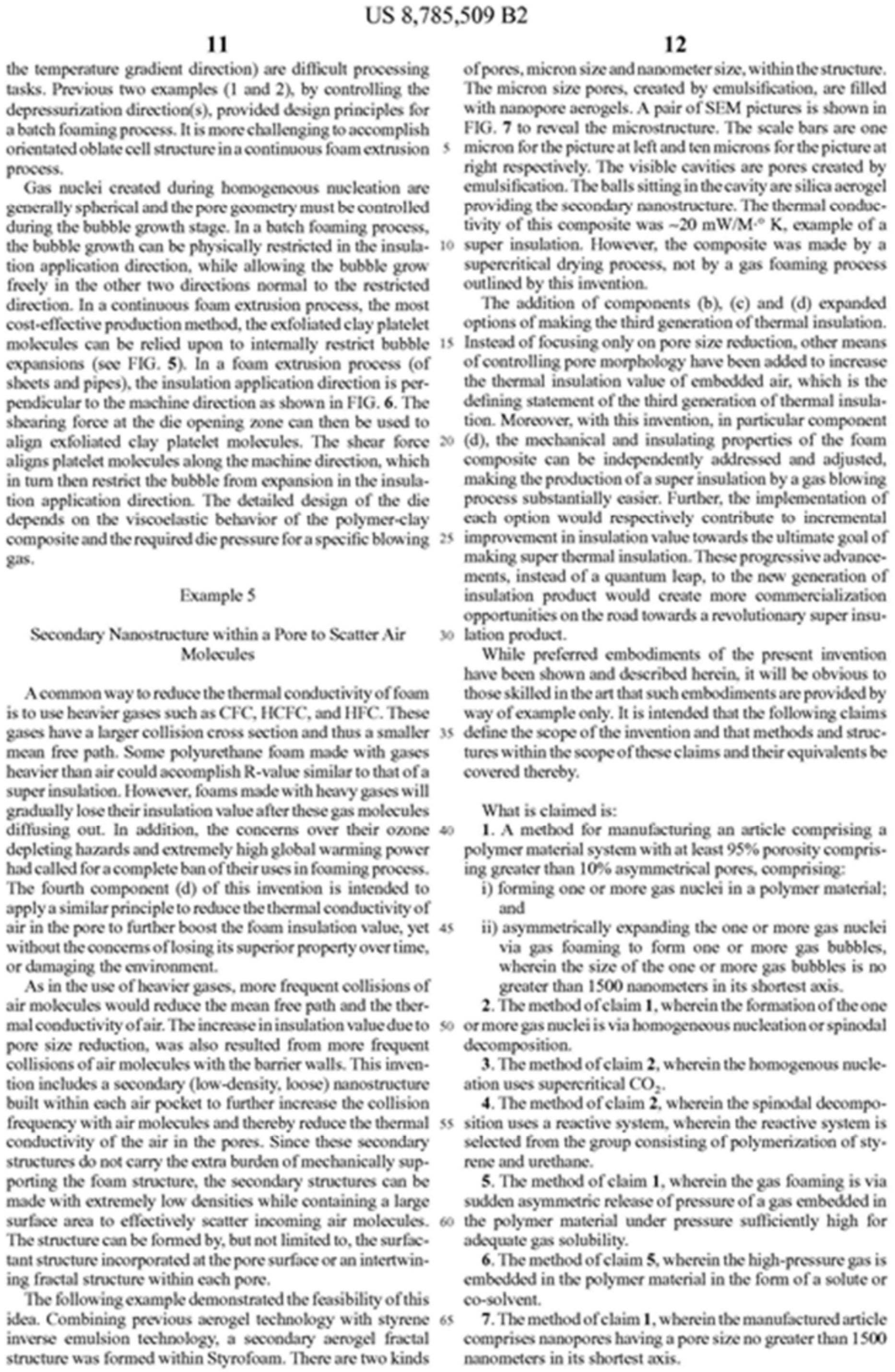

the temperature gradient direction) are difficult processing tasks. Previous two examples (1 and 2), by controlling the depressurization direction(s), provided design principles for a batch foaming process. It is more challenging to accomplish orientated oblate cell structure in a continuous foam extrusion process.

Gas nuclei created during homogeneous nucleation are generally spherical and the pore geometry must be controlled during the bubble growth stage. In a batch foaming process, the bubble growth can be physically restricted in the insulation application direction, while allowing the bubble grow freely in the other two directions normal to the restricted direction. In a continuous foam extrusion process, the most cost-effective production method, the exfoliated clay platelet molecules can be relied upon to internally restrict bubble expansions (see FIG. **5**). In a foam extrusion process (of sheets and pipes), the insulation application direction is perpendicular to the machine direction as shown in FIG. **6**. The shearing force at the die opening zone can then be used to align exfoliated clay platelet molecules. The shear force aligns platelet molecules along the machine direction, which in turn then restrict the bubble from expansion in the insulation application direction. The detailed design of the die depends on the viscoelastic behavior of the polymer-clay composite and the required die pressure for a specific blowing gas.

### Example 5

### Secondary Nanostructure within a Pore to Scatter Air Molecules

A common way to reduce the thermal conductivity of foam is to use heavier gases such as CFC, HCFC, and HFC. These gases have a larger collision cross section and thus a smaller mean free path. Some polyurethane foam made with gases heavier than air could accomplish R-value similar to that of a super insulation. However, foams made with heavy gases will gradually lose their insulation value after these gas molecules diffusing out. In addition, the concerns over their ozone depleting hazards and extremely high global warming power had called for a complete ban of their uses in foaming process. The fourth component (d) of this invention is intended to apply a similar principle to reduce the thermal conductivity of air in the pore to further boost the foam insulation value, yet without the concerns of losing its superior property over time, or damaging the environment.

As in the use of heavier gases, more frequent collisions of air molecules would reduce the mean free path and the thermal conductivity of air. The increase in insulation value due to pore size reduction, was also resulted from more frequent collisions of air molecules with the barrier walls. This invention includes a secondary (low-density, loose) nanostructure built within each air pocket to further increase the collision frequency with air molecules and thereby reduce the thermal conductivity of the air in the pores. Since these secondary structures do not carry the extra burden of mechanically supporting the foam structure, the secondary structures can be made with extremely low densities while containing a large surface area to effectively scatter incoming air molecules. The structure can be formed by, but not limited to, the surfactant structure incorporated at the pore surface or an intertwining fractal structure within each pore.

The following example demonstrated the feasibility of this idea. Combining previous aerogel technology with styrene inverse emulsion technology, a secondary aerogel fractal structure was formed within Styrofoam. There are two kinds of pores, micron size and nanometer size, within the structure. The micron size pores, created by emulsification, are filled with nanopore aerogels. A pair of SEM pictures is shown in FIG. **7** to reveal the microstructure. The scale bars are one micron for the picture at left and ten microns for the picture at right respectively. The visible cavities are pores created by emulsification. The balls sitting in the cavity are silica aerogel providing the secondary nanostructure. The thermal conductivity of this composite was ~20 mW/M·° K, example of a super insulation. However, the composite was made by a supercritical drying process, not by a gas foaming process outlined by this invention.

The addition of components (b), (c) and (d) expanded options of making the third generation of thermal insulation. Instead of focusing only on pore size reduction, other means of controlling pore morphology have been added to increase the thermal insulation value of embedded air, which is the defining statement of the third generation of thermal insulation. Moreover, with this invention, in particular component (d), the mechanical and insulating properties of the foam composite can be independently addressed and adjusted, making the production of a super insulation by a gas blowing process substantially easier. Further, the implementation of each option would respectively contribute to incremental improvement in insulation value towards the ultimate goal of making super thermal insulation. These progressive advancements, instead of a quantum leap, to the new generation of insulation product would create more commercialization opportunities on the road towards a revolutionary super insulation product.

While preferred embodiments of the present invention have been shown and described herein, it will be obvious to those skilled in the art that such embodiments are provided by way of example only. It is intended that the following claims define the scope of the invention and that methods and structures within the scope of these claims and their equivalents be covered thereby.

What is claimed is:

**1**. A method for manufacturing an article comprising a polymer material system with at least 95% porosity comprising greater than 10% asymmetrical pores, comprising:
- i) forming one or more gas nuclei in a polymer material; and
- ii) asymmetrically expanding the one or more gas nuclei via gas foaming to form one or more gas bubbles, wherein the size of the one or more gas bubbles is no greater than 1500 nanometers in its shortest axis.

**2**. The method of claim **1**, wherein the formation of the one or more gas nuclei is via homogeneous nucleation or spinodal decomposition.

**3**. The method of claim **2**, wherein the homogenous nucleation uses supercritical $CO_2$.

**4**. The method of claim **2**, wherein the spinodal decomposition uses a reactive system, wherein the reactive system is selected from the group consisting of polymerization of styrene and urethane.

**5**. The method of claim **1**, wherein the gas foaming is via sudden asymmetric release of pressure of a gas embedded in the polymer material under pressure sufficiently high for adequate gas solubility.

**6**. The method of claim **5**, wherein the high-pressure gas is embedded in the polymer material in the form of a solute or co-solvent.

**7**. The method of claim **1**, wherein the manufactured article comprises nanopores having a pore size no greater than 1500 nanometers in its shortest axis.

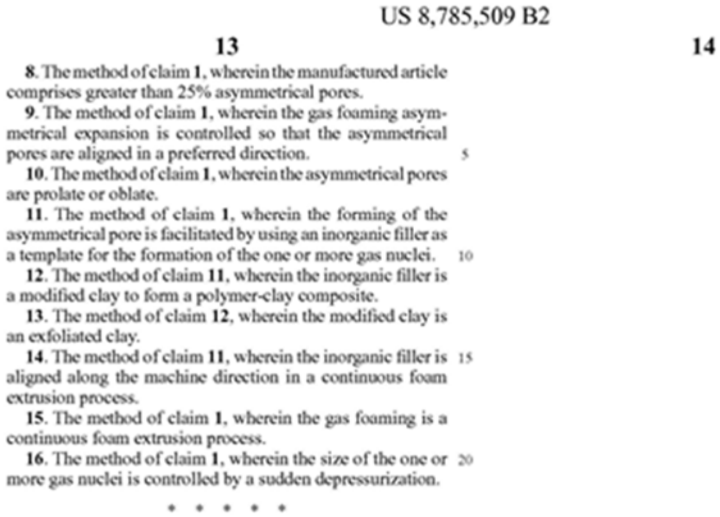

US 8,785,509 B2

13

14

**8**. The method of claim **1**, wherein the manufactured article comprises greater than 25% asymmetrical pores.

**9**. The method of claim **1**, wherein the gas foaming asymmetrical expansion is controlled so that the asymmetrical pores are aligned in a preferred direction.

**10**. The method of claim **1**, wherein the asymmetrical pores are prolate or oblate.

**11**. The method of claim **1**, wherein the forming of the asymmetrical pore is facilitated by using an inorganic filler as a template for the formation of the one or more gas nuclei.

**12**. The method of claim **11**, wherein the inorganic filler is a modified clay to form a polymer-clay composite.

**13**. The method of claim **12**, wherein the modified clay is an exfoliated clay.

**14**. The method of claim **11**, wherein the inorganic filler is aligned along the machine direction in a continuous foam extrusion process.

**15**. The method of claim **1**, wherein the gas foaming is a continuous foam extrusion process.

**16**. The method of claim **1**, wherein the size of the one or more gas nuclei is controlled by a sudden depressurization.

* * * * *